

Improving tide-estuary representation in MPAS-Ocean: progress and outlook

Joseph Zhang

Virginia Institute of Marine Science

Zhengui Wang, Fei Chai

University of Maine

October 4, 2018



Overview

- Review of proposed tasks & timeline
- MPAS-OI: a new nearshore component for MPAS-Ocean
- SCHISM: another nearshore model for coupling to MPAS-O
- Model coupling work (ongoing)

Proposed tasks

The overarching goal of this research is to produce a skill-assessed tide-estuary representation, including BGC components of the ecosystem, into the MPAS-O global climate modeling system. For the BGC model development, we will focus on carbon and nutrient cycling in TES, and how they affect open-ocean carbon cycle dynamics.

- Hydro**
- Task 1: Benchmark MPAS-O with a few TES
 - Task 2: Add a new turbulence closure model suitable for TES
 - *Task 3: Implement an implicit time-stepping scheme: **MPAS-OI & coupling**
 - Task 4: Add orthogonal triangular-quadrangular cells for TES
 - Task 5: Add an alternative scheme for momentum advection
 - Task 6: Improve bottom representation (ghost-cell Immersed Boundary Method; alternate: **sub-grid bathymetry**)
 - Task 7: Implement implicit vertical transport solver
 - Task 8: Work on inundation scheme (nonlinear iterative solver)
 - Task 9: Incorporate SCHISM into MPAS-O
 - Task 10: Validate the improved TES model(s) and document the metrics

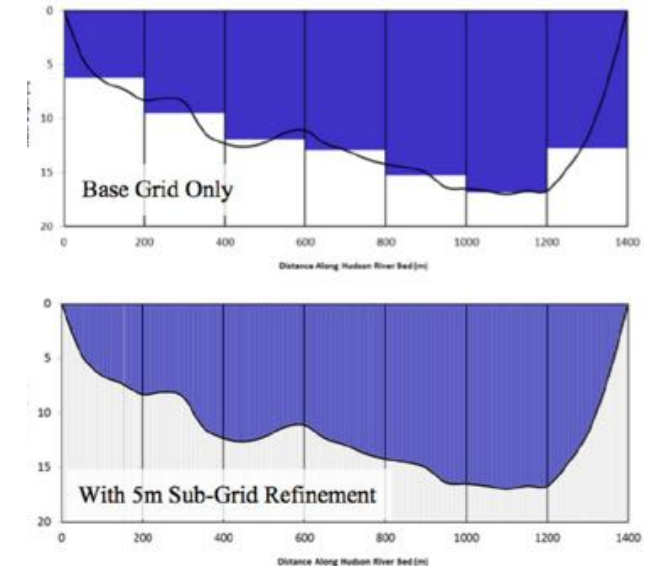
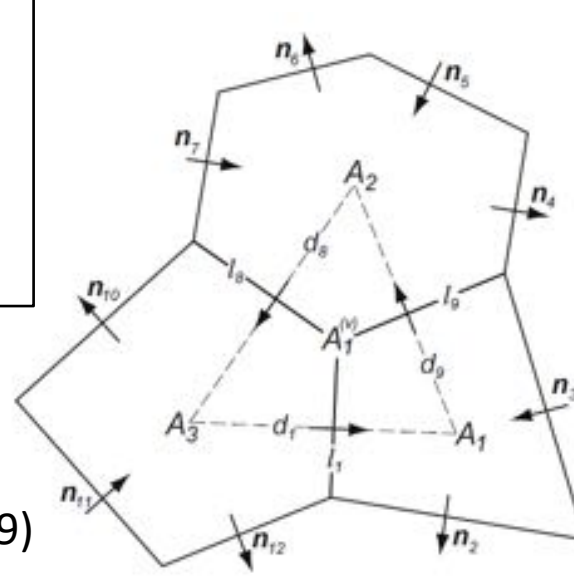
- BGC**
- Task 11: Implement and refine carbon cycle model within MPAS-OI
 - Task 12: Refine the role of phosphorus in MPAS-OI/BGC
 - Task 13: Improve light treatment in MPAS-OI/BGC
 - Task 14: Validate MPAS-OI/BGC for other TES
 - Task 15: Deliver final code, documentation and annual reports

Timeline



MPAS-OI: a nearshore component of global MPAS-Ocean

- Bridge the gap between global ocean model and estuaries & rivers
 - Both SCHISM and MPAS-OI are being coupled to MPAS-O
- Formulation based on the subgrid, FV solver of UnTRIM (Casulli 2009), but with MPAS' approach for conservation of energy and potential vorticity, i.e. Thuburn et al. (2009) approach to reconstruct the tangential velocity
- The core is a semi-implicit, nonlinear solver for coupled continuity and momentum equation on **orthogonal** grids
 - The convergence of the nonlinear solver is always guaranteed
 - Mass conservative wetting and drying with arbitrary time steps with positivity guaranteed
 - Subgrid capability for better representation of high-resolution bathymetry as in LiDAR: great for storm surge applications
 - Enables fast & accurate prediction of street/building level inundation
- Grid quality is a key (more later)

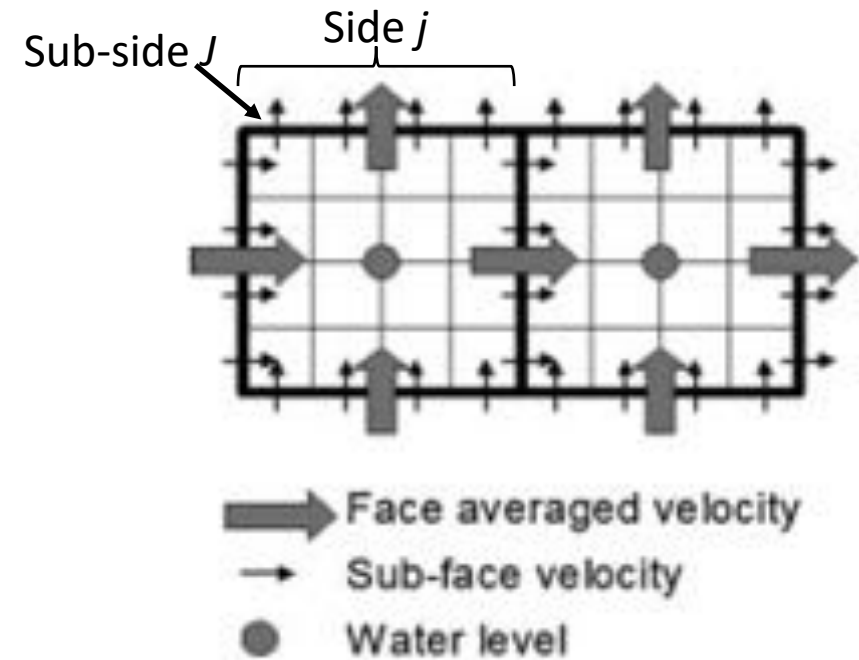


Thuburn et al. (2009)

Core nonlinear solver

$$\begin{cases} H_t + \nabla \cdot \int_{-h}^{\eta} \mathbf{u} dz = 0 \\ \frac{D\mathbf{u}}{Dt} = -g\nabla\eta + \frac{\partial}{\partial z} \left(v \frac{\partial \mathbf{u}}{\partial z} \right) + \mathbf{f} \end{cases} \quad \text{explicit}$$

$$\begin{cases} v \frac{\partial \mathbf{u}}{\partial z} = \boldsymbol{\tau}_w, & z = \eta \\ v \frac{\partial \mathbf{u}}{\partial z} = \chi \mathbf{u}_b, & z = -h \end{cases}$$



- *Arbitrary* orthogonal polygon in the horizontal dimension, with each element cell sub-divided into 'sub-grid' cells
- Z coordinates in the vertical
- Define normal velocity at a sub-side (j,J) and a vertical layer k as $u(j,J,k)$, and the discretized momentum eq is

$$\Delta z_{j,J,k}^n u_{j,J,k}^{n+1} = G_{j,J,k}^n - g\theta \Delta t \frac{\eta_{(j,2)}^{n+1} - \eta_{(j,1)}^{n+1}}{\delta_j} + \Delta t \left[v_{j,k+1/2}^n \frac{u_{j,J,k+1}^{n+1} - u_{j,J,k}^{n+1}}{\Delta z_{j,J,k+1/2}^n} - v_{j,k-1/2}^n \frac{u_{j,J,k}^{n+1} - u_{j,J,k-1}^{n+1}}{\Delta z_{j,J,k-1/2}^n} \right]$$

explicit

$(k = m_{j,J+1}, \dots, M_j^n; j = 1, \dots, N_s)$

Matrix form:

$$A_{j,J} U_{j,J}^{n+1} = G_{j,J} - g\theta \frac{\Delta t}{\delta_j} [\eta_{(j,2)}^{n+1} - \eta_{(j,1)}^{n+1}] \Delta z_{j,J}^n$$

Core nonlinear solver

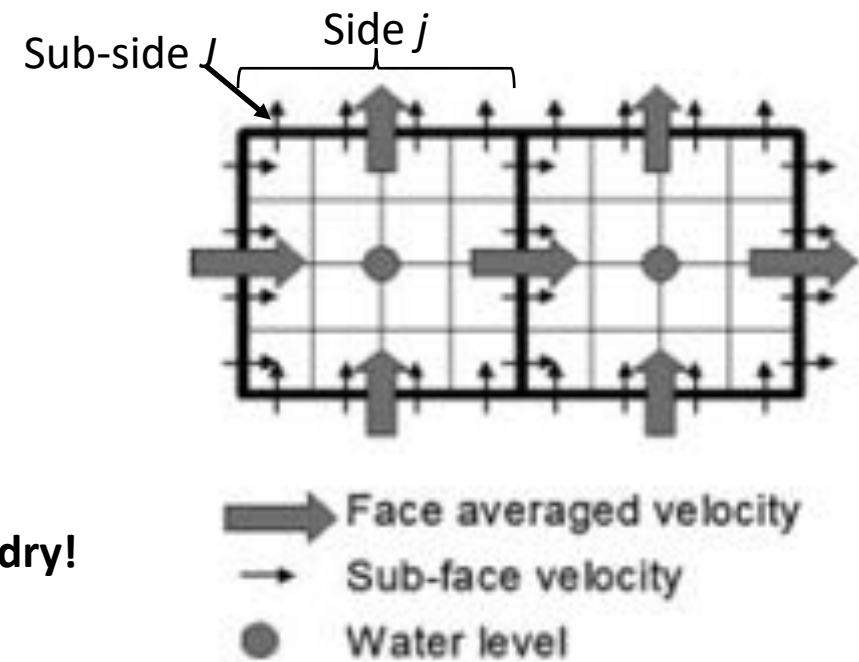
FV discretization of the continuity eq for a cell i is:

$$V_i(\eta_i^{n+1}) = V_i(\eta_i^n) - \Delta t \sum_j s_{i,j} \sum_J \lambda_{j,J} [\Delta Z_{j,J}^n]^T [\theta U_{j,J}^{n+1} + (1 - \theta) U_{j,J}^n]$$

where the volume takes into account the **partially** dry cell:

$$V_i(\eta_i^n) = \int_{\Omega_i} \max[0, h + \eta_i^n] d\Omega_i$$

← **Guarantees positivity in wet/dry!**



Substituting the momentum eq into continuity eq gives the final weakly nonlinear equation for unknown elevations:

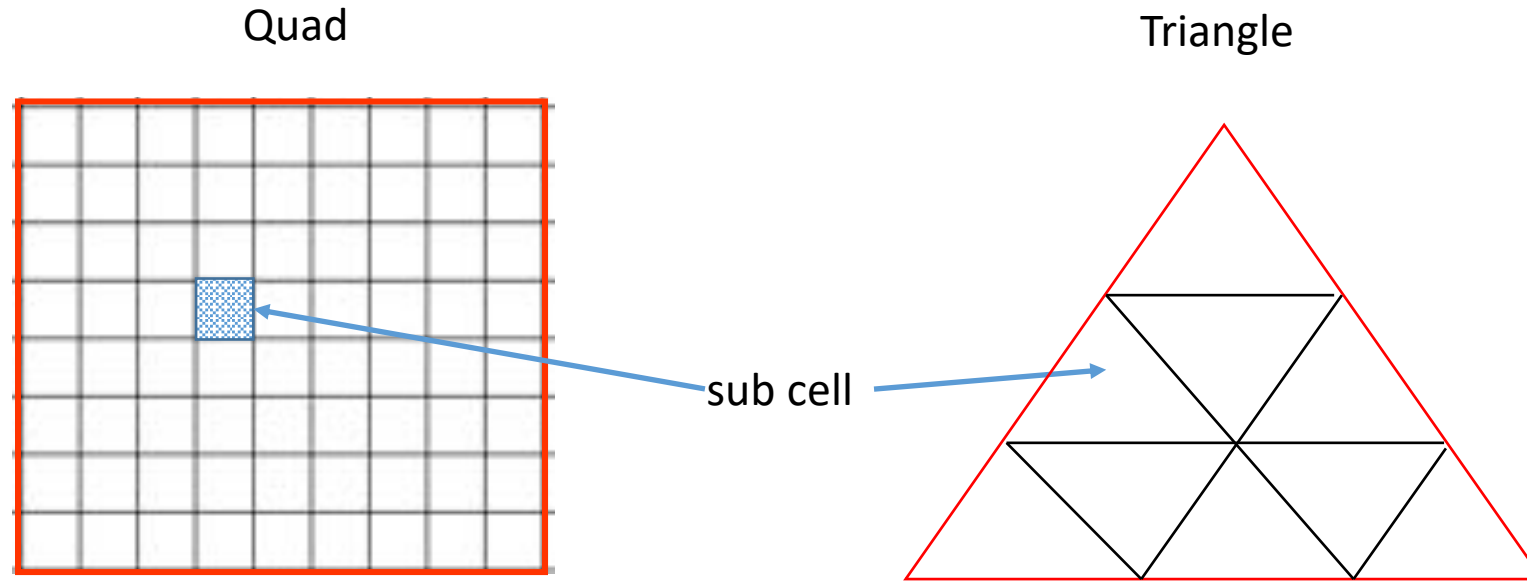
$$V_i(\eta_i^{n+1}) - g\theta^2\Delta t^2 \sum_j \psi_j \frac{\eta_{(i,j)}^{n+1} - \eta_i^{n+1}}{\delta_j} = b_i \quad (i = 1, \dots, N_e)$$

$$\psi_j = \sum_J \lambda_{j,J} [\Delta Z_{j,J}^n]^T A_{j,J}^{-1} \Delta Z_{j,J}^n$$

← Cell center distance

- The weakly nonlinear eq is solved using a quasi Newton iteration method (and convergence is fast and guaranteed)
- In the absence of wetting and drying, the iteration converges in 1 iteration
- **The scheme enforces strict positivity and mass conservation, and allows partial wetting during inundation process, with any time steps!**

Sub-grid bathymetry



- * High-resolution DEM (e.g. LiDAR) to populate the sub-grid depths
- * At the moment we have not implemented sub-grids for other types of polygons, due to difficulty in generating good-quality orthogonal grids using those polygons. However, a subgrid discretization is doable for any polygonal cells

Transport: TVD²

Solve the transport eq in 3 sub-steps:

$$\left\{ \begin{array}{l} C_i^{m+1} = C_i^n + \frac{\Delta t_m}{V_i} \sum_{j \in S_H^-} |Q_j| (C_j^m - C_i^m) - \frac{\Delta t_m}{V_i} \sum_{j \in S_H} Q_j \hat{\psi}_j^m, \quad (m = 1, \dots, M) \\ \tilde{C}_i = C_i^{M+1} + \frac{\Delta t}{V_i} \sum_{j \in S_V^-} |Q_j| (\tilde{C}_j - \tilde{C}_i) - \frac{\Delta t}{V_i} \sum_{j \in S_V} Q_j (\Phi_j + \Psi_j), \quad (j = k_b, \dots, N_z) \\ C_i^{n+1} = \tilde{C}_i + \frac{A_i \Delta t}{V_i} \left[\left(\kappa \frac{\partial C}{\partial z} \right)_{i,k}^{n+1} - \left(\kappa \frac{\partial C}{\partial z} \right)_{i,k-1}^{n+1} \right] + \frac{\Delta t}{V_i} \int_{V_i} F_h^n dV, \quad (k = k_b, \dots, N_z) \end{array} \right.$$

Horizontal advection
(explicit TVD method)

Vertical advection (implicit TVD²)

Remaining (implicit diffusion, settling)

- 1st step: explicit TVD
- 2nd step: Taylor expansion in space *and* time

$$C_j^{n+1/2} = C_{jup}^{n+1} + \Phi_j + \Psi_j = C_{jup}^{n+1} + \mathbf{r} \bullet [\nabla C]_{jup}^{n+1} - \frac{\Delta t}{2} \left[\frac{\partial C}{\partial t} \right]_{jup}^{n+1}$$

↑Space limiter
 ↑Time limiter

Duraisamy and Baeder (2007)

TVD²

$$\tilde{C}_i + \frac{\frac{\Delta t}{V_i} \sum_{j \in S_V^-} |Q_j| \left[1 + \frac{1}{2} \left(\sum_{p \in S_V^+} \frac{\phi_p}{r_p} - \phi_j \right) \right] (\tilde{C}_i - \tilde{C}_j)}{1 + \frac{\Delta t}{2V_i} \sum_{j \in S_V^+} |Q_j| \left(\sum_{q \in S_V^-} \frac{\psi_q}{s_q} - \psi_j \right)} = C_i^{M+1}$$

Upwind ratio $r_p = \frac{\sum_{q \in S_V^-} |Q_q| (\tilde{C}_q - \tilde{C}_i)}{|Q_p| (\tilde{C}_i - \tilde{C}_p)}, p \in S_V^+$

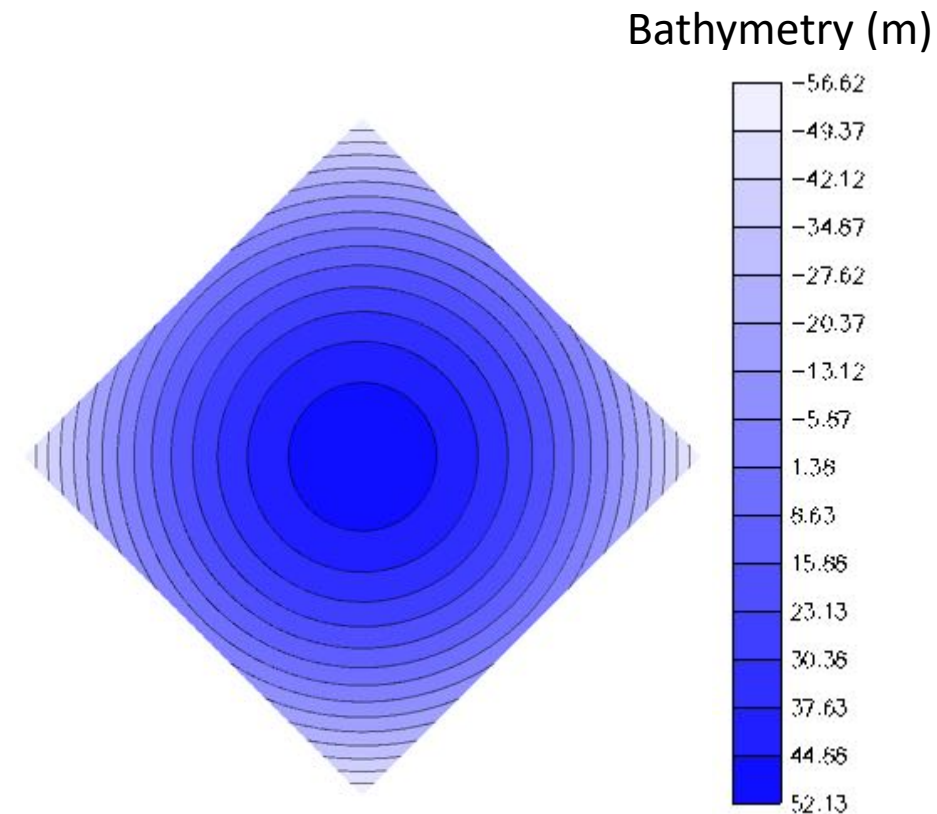
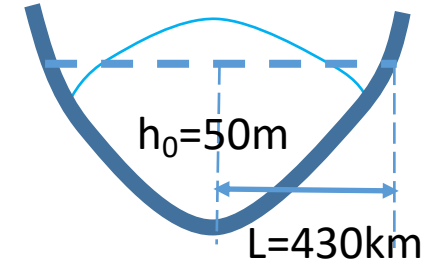
Downwind ratio $s_q = \frac{(\tilde{C}_i - C_i^{M+1}) \sum_{p \in S_V^+} |Q_p|}{|Q_q| (\tilde{C}_q - C_q^{M+1})}, q \in S_V^-$

TVD condition: $\left[\begin{array}{l} 1 + \frac{1}{2} \left(\sum_{p \in S_V^+} \frac{\phi_p}{r_p} - \phi_j \right) \geq 0 \\ 1 + \frac{\Delta t}{2V_i} \sum_{j \in S_V^+} |Q_j| \left(\sum_{q \in S_V^-} \frac{\psi_q}{s_q} - \psi_j \right) \geq \delta > 0 \quad (\text{iterative solver}) \end{array} \right.$

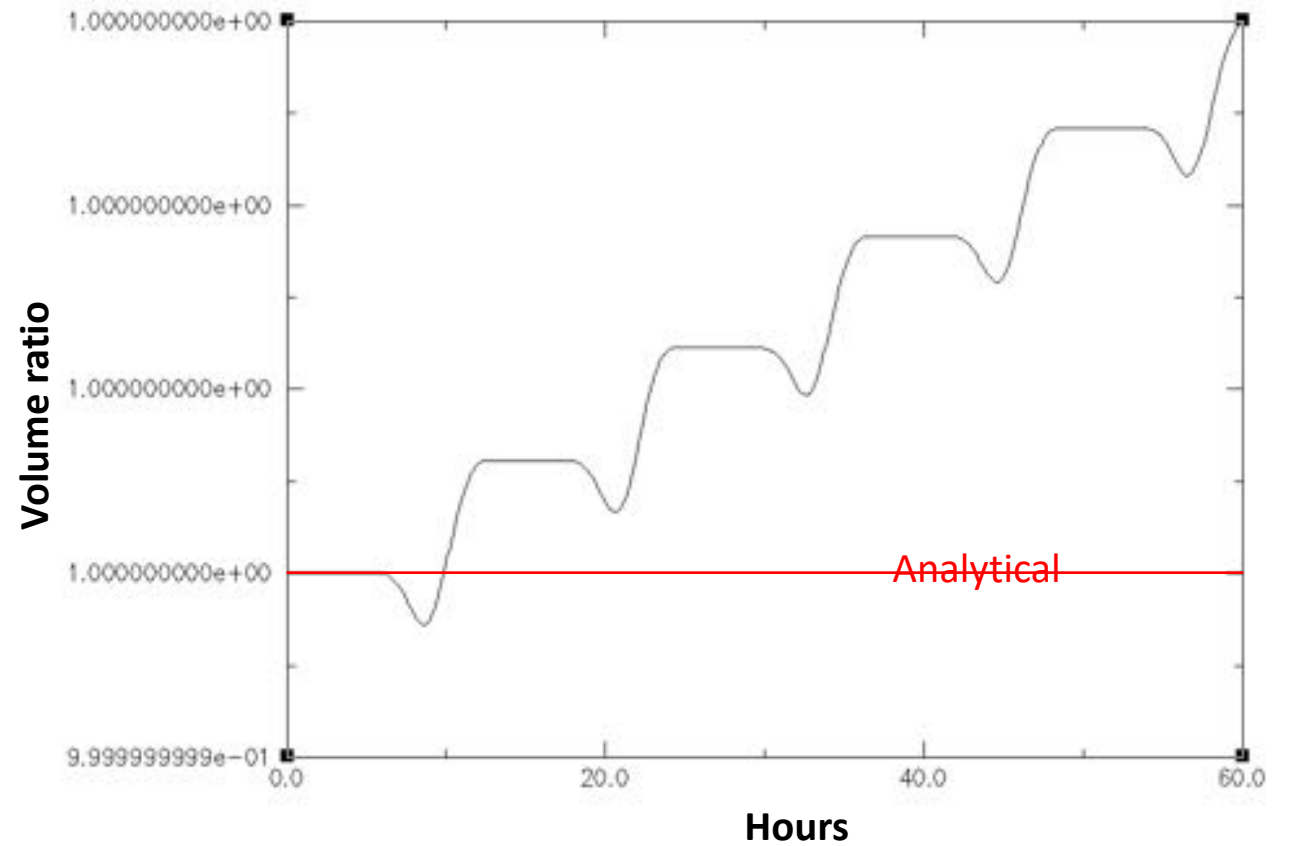
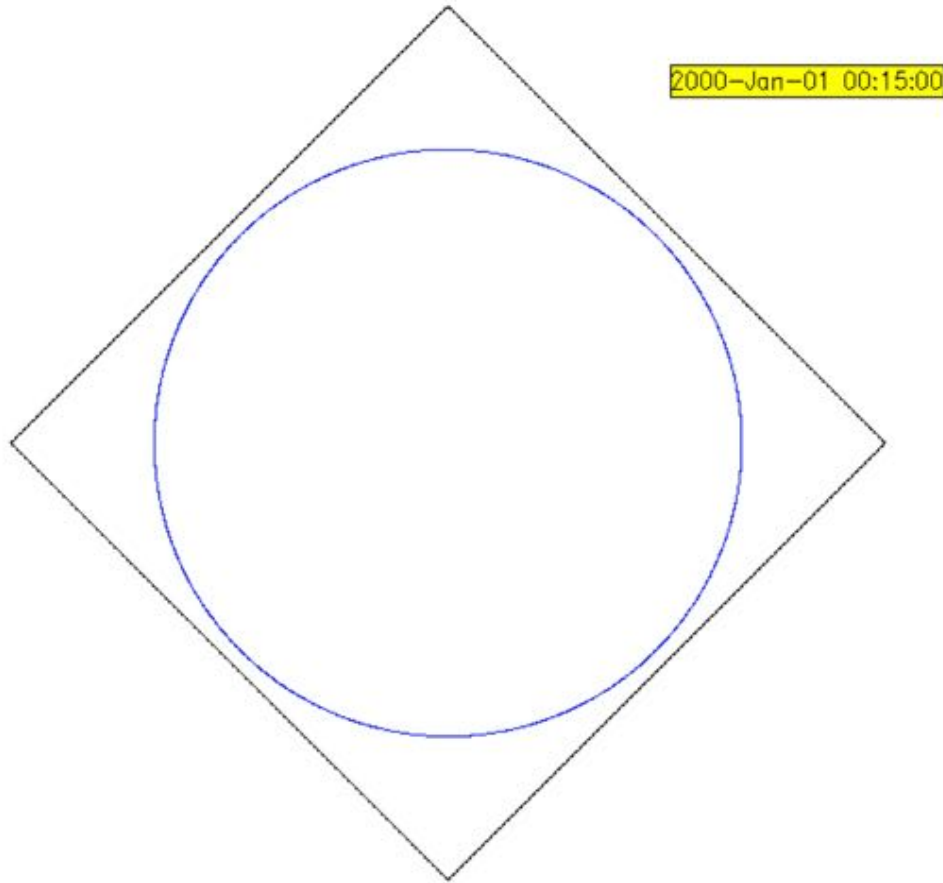
- Iterative solver converges very fast
- 2nd-order accurate in space *and time*
- Monotone
- Alleviate the sub-cycling/small Δt for transport that plagued explicit TVD; good news for the **thin layer syndrome!**
- Can be used at any depths

Model benchmark: inundation test on a parabolic bowl

- Thacker's parabolic bowl test
 - One of few existing analytical solutions for nonlinear shallow-water equation with inundation
 - Radially symmetric inundation; no bottom friction
 - Used Casulli's (2009) configuration: depth $h=h_0(1-r^2/L^2)$, amplitude $\eta_0=2\text{m}$, resulting in period $T\sim 12\text{h}$, and min/max shoreline radii of 422 and 439km
 - All boundaries are closed; motion driven by sloshing due to initial displacement (potential energy): good test for energy conservation also
- Model set-up ('base')
 - Uniform quad grid resolution = 2km; 1 vertical layer
 - Domain rotated to test robustness
 - $N_{\text{sub}}=5$ (so 400m at sub-grid level)
 - $\Delta t=300\text{s}$; $\theta=0.51$
 - Nonlinear solver
- Sensitivity test wrt
 - ✓ Δt
 - ✓ θ
 - ✓ Vertical grid
 - ✓ # of sub-grid divisions
 - ✓ Reconstruction of tangential vel using simple averaging
 - ✓ Linear solver

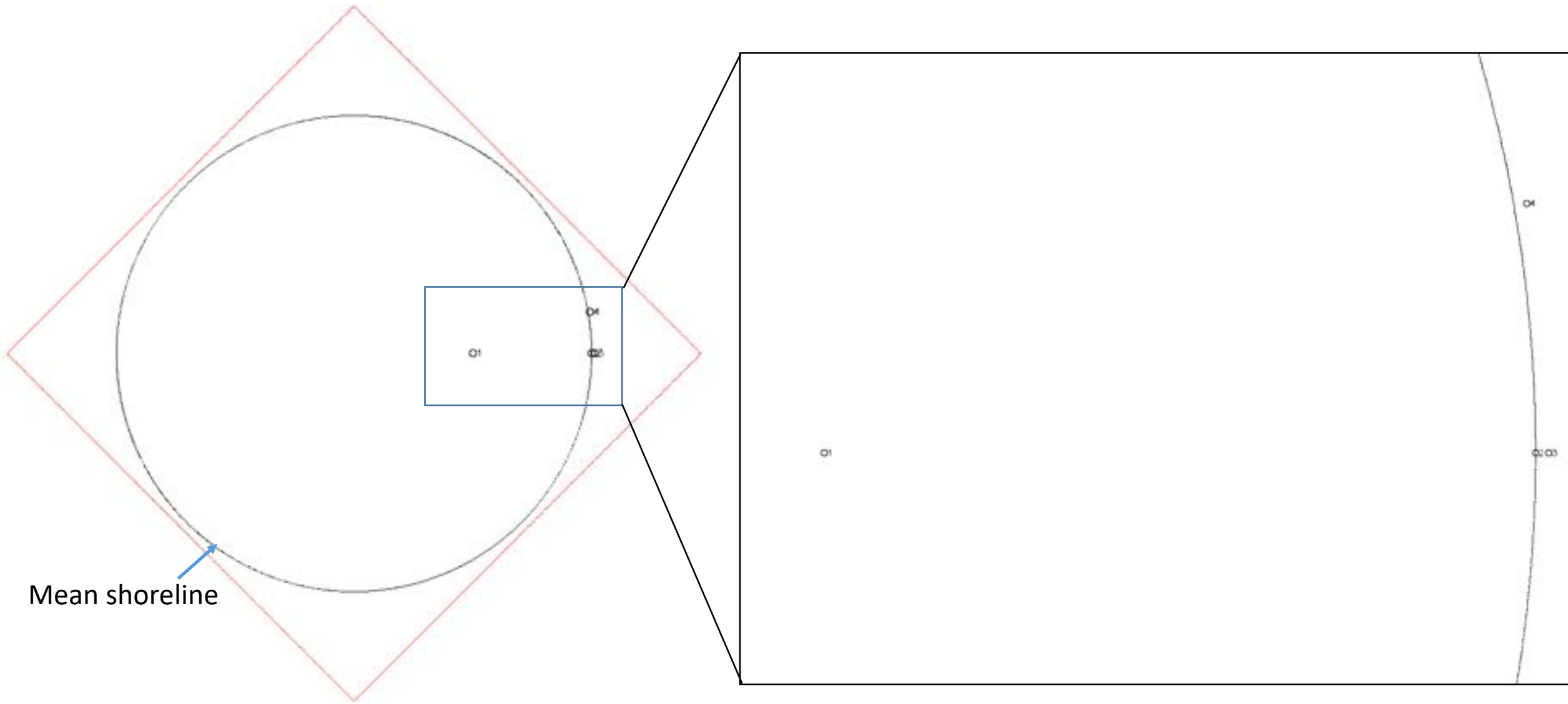


Model benchmark (2): inundation test on a parabolic bowl



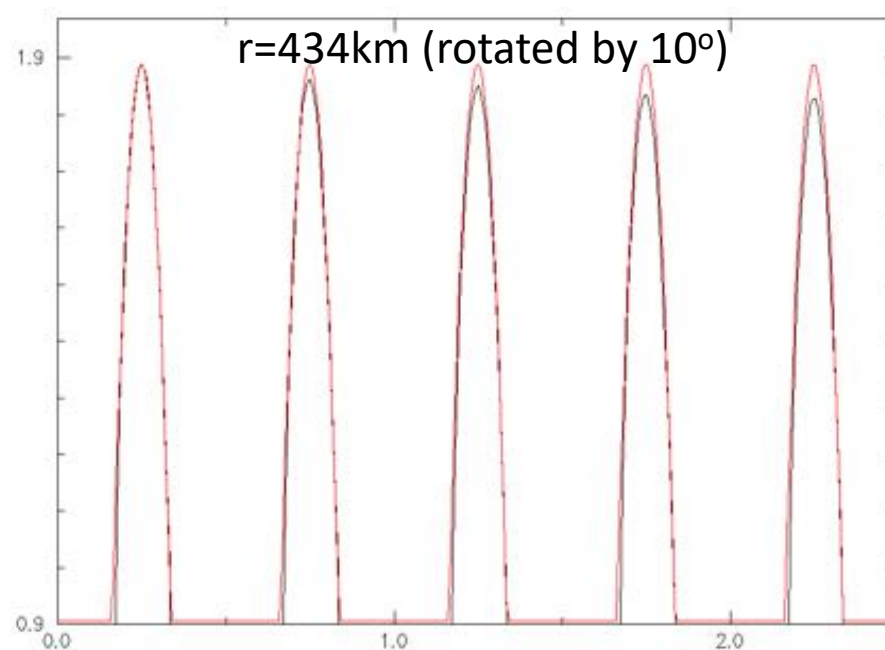
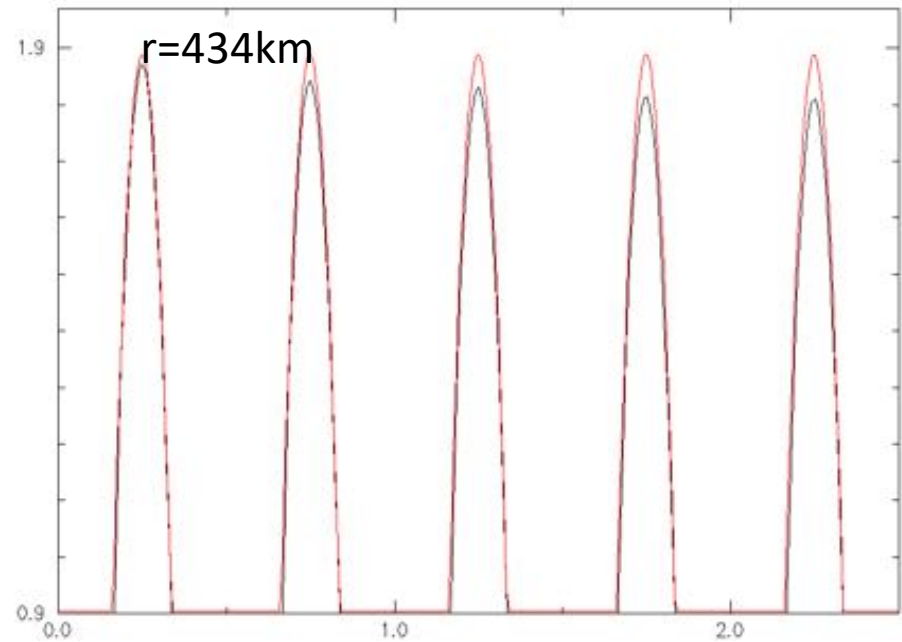
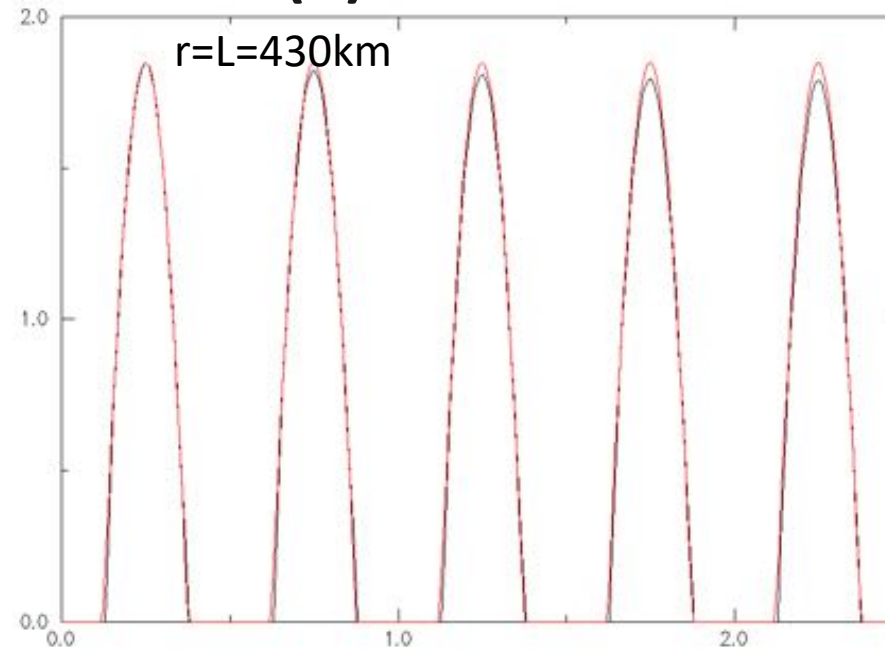
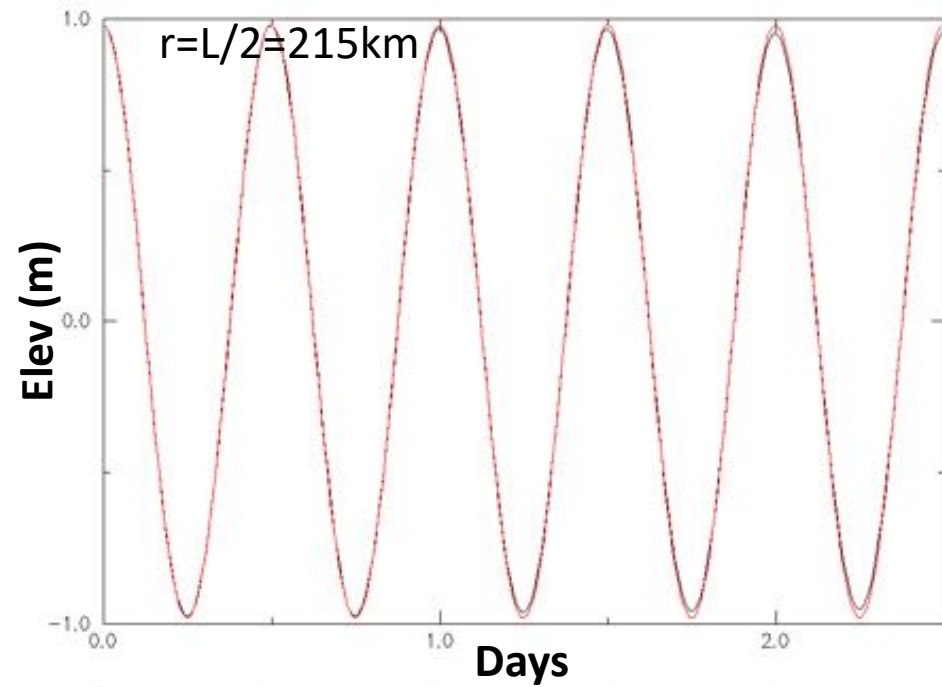
- Results are mostly symmetric
- Total volume is conserved within machine precision despite strong wetting and drying

Model benchmark (2): time series stations



- Station 4 is located at a same circle as Station 3 (azimuth=10°). It is used to test radial symmetry

Model benchmark (2): elev time series

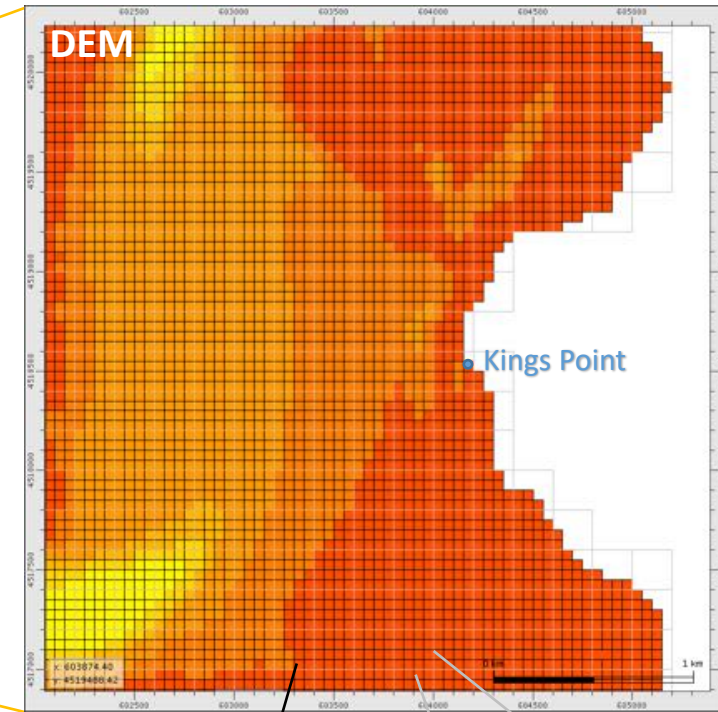
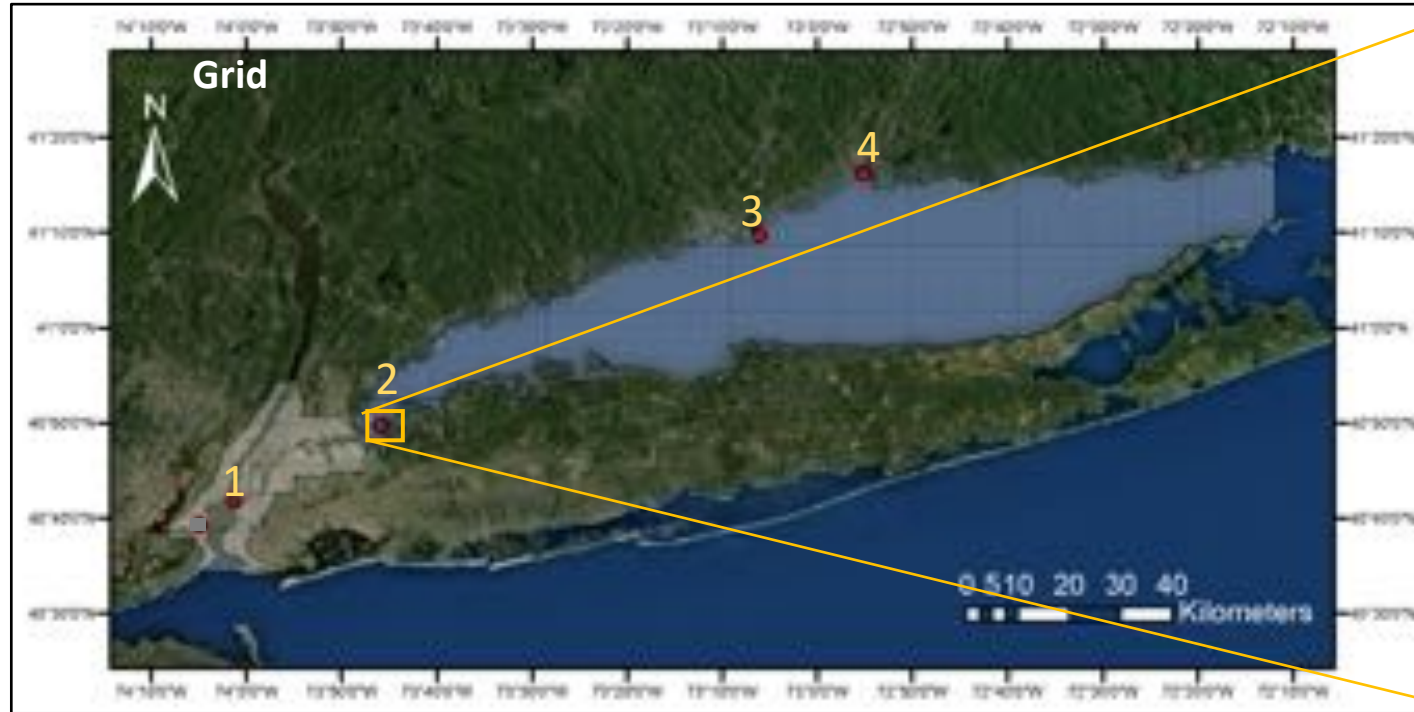


Model DATA

- Model results show slight damping
- The results are satisfactory inside the inundation zone
- Radial symmetry is preserved
- Efficiency is ensured with large time step!

Storm surge and inundation modeling during Hurricane Sandy in 2012

1. Model domain (shaded area) and 4 water level gauges



Station Number	1	2	3	4
Station Name	The Battery, NY	Kings Point, NY	Bridgeport, CT	New Haven, CT

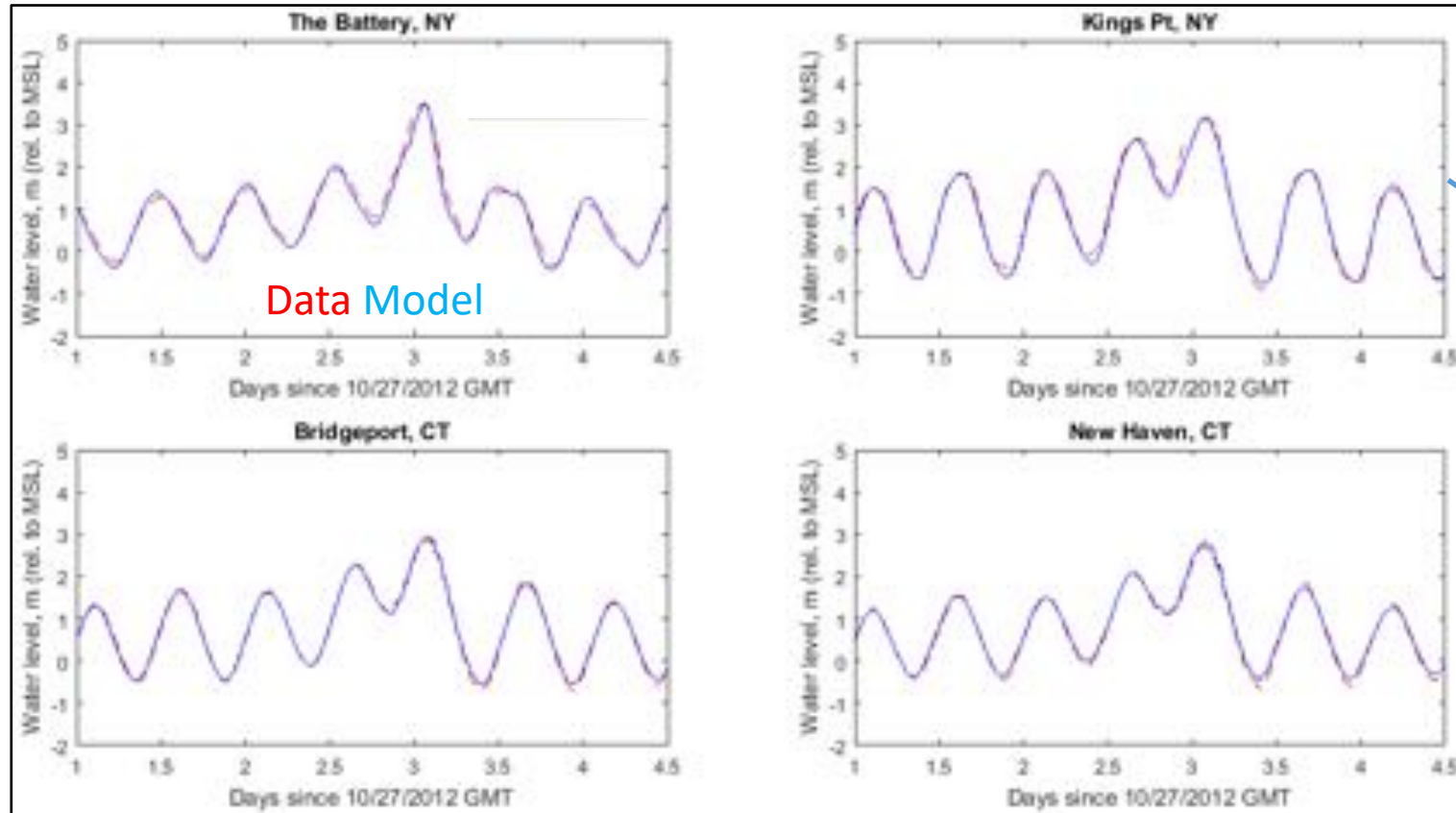
Sub-grid
5 X 5 m

Base Grid
200 X 200 m

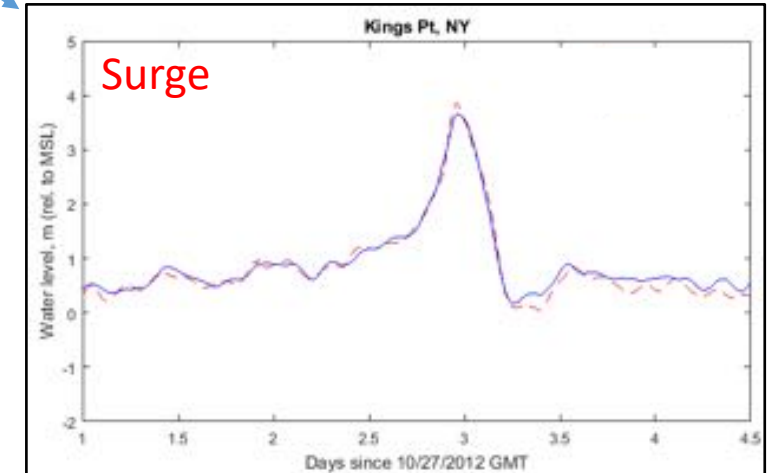
2. Model setup

- Structured (square) grid: 88k nodes, 90k elements (base), 200m base grid resolution. 5m subgrid resolution
- DEM: 5m resolution LIDAR over NYC, 10m-90m coastal relief model over Long Island Sound
- Open boundary: South and East: NOAA observed water level; North: river discharge in Hudson (also tried info from large-scale SCHISM model)
- Atmospheric forcing: wind and pressure measurement at Bridgeport, CT; uniform across the domain.
- **Efficiency: 2D run, $\Delta t=180s$, 80 Intel Broadwell cores, 10-day run (10/22-11/01/2012) completed in 20min (720 x real time speedup).** For this large domain, UnTRIM2 would need more than 360min to finish.

Storm tide results compared with NOAA observation



The model was able to accurately catch the abrupt surge at Kings Point, NY. The maximum surge was almost 4 m (the highest among all stations).



Statistics

Station	The Battery	Kings Point	Bridgeport	New Haven
R ²	0.97	0.97	0.98	0.98
RMSE (cm)	12.6	11.1	5.7	7.5
MAE (cm)	10.5	8.5	4.3	5.8

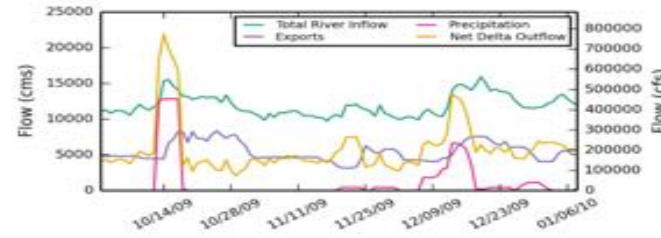
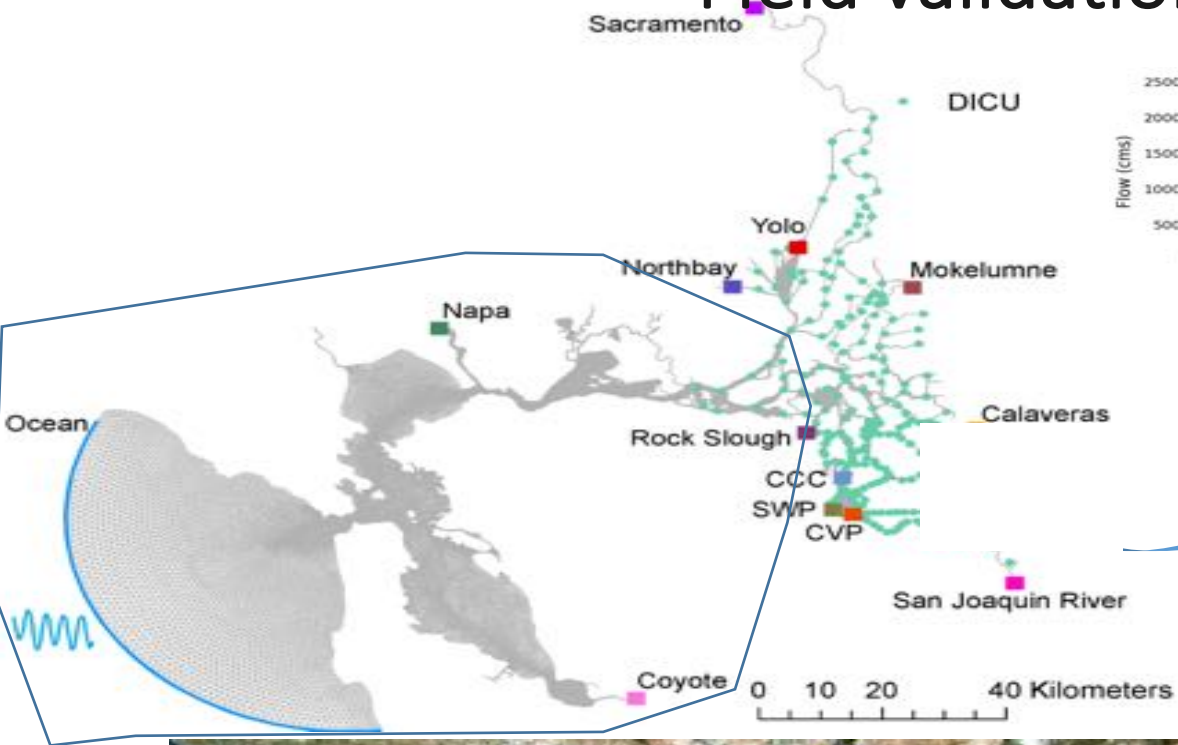
RMSE: Root-Mean-Square-Error; MAE: Mean Absolute Error

4. Modeled maximum flooding extent compared with FEMA Map
Zoom-in near the southern tip of Manhattan.

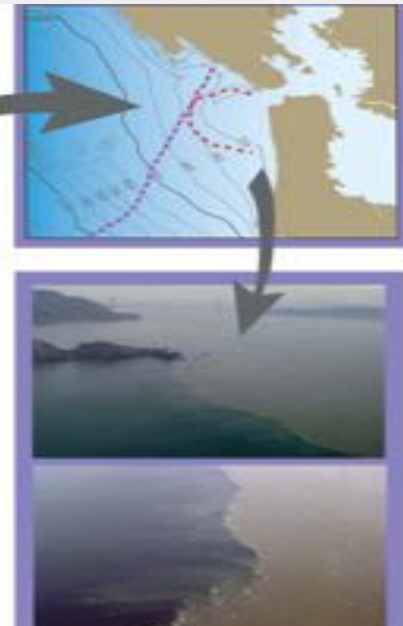


Overall, the modeled inundation matched approximately 75% with FEMA street-level map around NJ and NY. The average error for the high water mark is on the order of 10 cm.

Field validation: San Francisco Bay



NDO



Field validation: San Francisco Bay

- * Bay-only grid (without Delta)
- * More complex geometry presented huge challenges for grid generator
 - * Over 10 different grids generated with JANET® (also time consuming: each grid took ~1 week)
- * Model set-up
 - * NARR wind; tides from WEBTIDES. T=const. S i.c. from USGS survey
 - * $\Delta t = 180 \text{ sec}$; $k-\omega$ closure. $N_z = 37$ (~1m vertical resolution near surface)
 - * Thuburn method is relaxed at the land boundary due to insufficient mesh quality there to avoid instability
 - * Simple averaging option works fine and gave comparable results (energy conservation is less of an issue in estuary)

Orthogonality Analysis

Deviation from Orthogonality (DO)

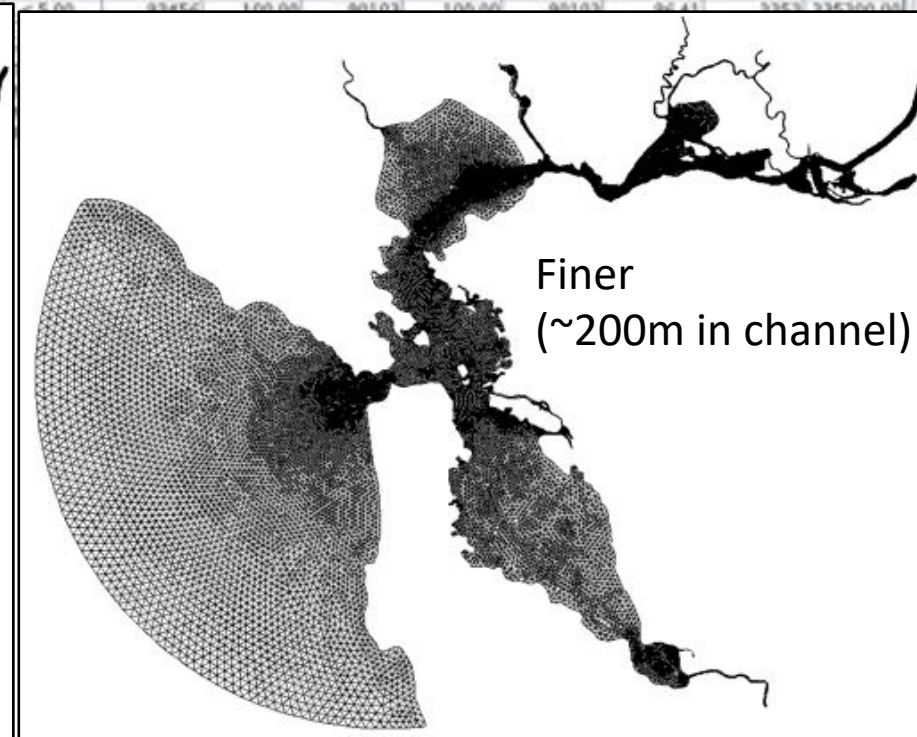
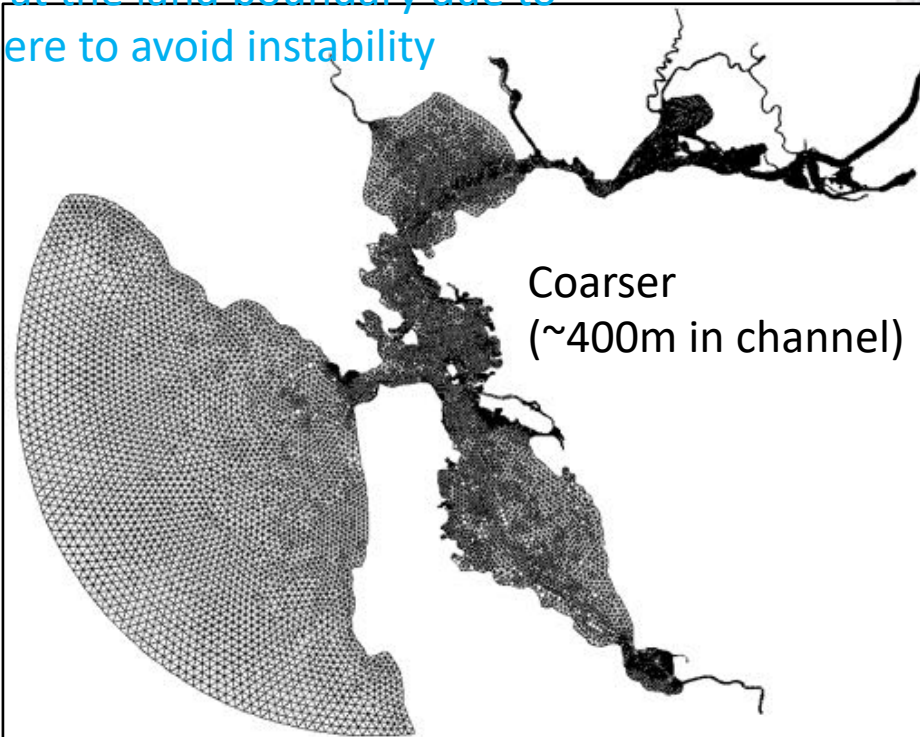
Max DO,TE = 46.65688 ° Max DO,NBE = 46.65688 ° Max DO,NPE = 46.65688 ° Max DO,PE = -1.00000 °
 Mean DO,TE = 0.01513 ° Mean DO,NBE = 0.01161 ° Mean DO,NPE = 0.01513 ° Mean DO,PE = 0.00000 °

	#TE	%	#NBE	%	#NPE	%	#PE	%
DO < 0.1 °	96949	99.81	87620	99.85	96949	99.81	0	0.00
DO < 0.5 °	96949	99.81	87620	99.85	96949	99.81	0	0.00
DO < 1.0 °	96949	99.81	87620	99.85	96949	99.81	0	0.00
DO < 5.0 °	96949	99.81	87620	99.85	96949	99.81	0	0.00
DO < 10...	96949	99.81	87620	99.85	96949	99.81	0	0.00
DO < 20...	96949	99.81	87620	99.85	96949	99.81	0	0.00
DO < 45...	96949	99.81	87620	99.85	96949	99.81	0	0.00
DO < 90...	96949	99.81	87620	99.85	96949	99.81	0	0.00

Centerpoint-Edge-Ratio of Adjacent Triangles (R)

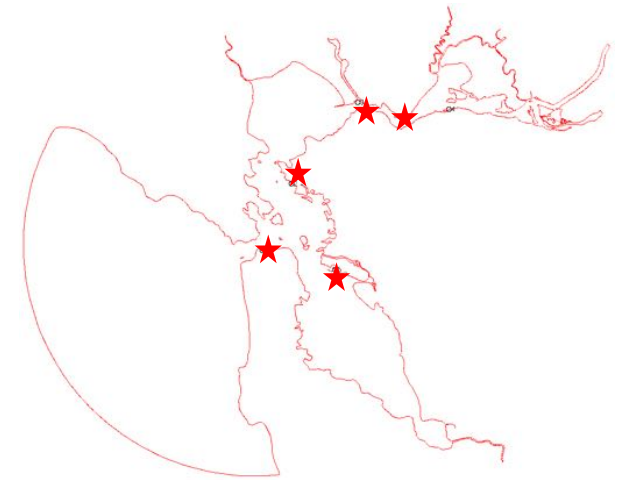
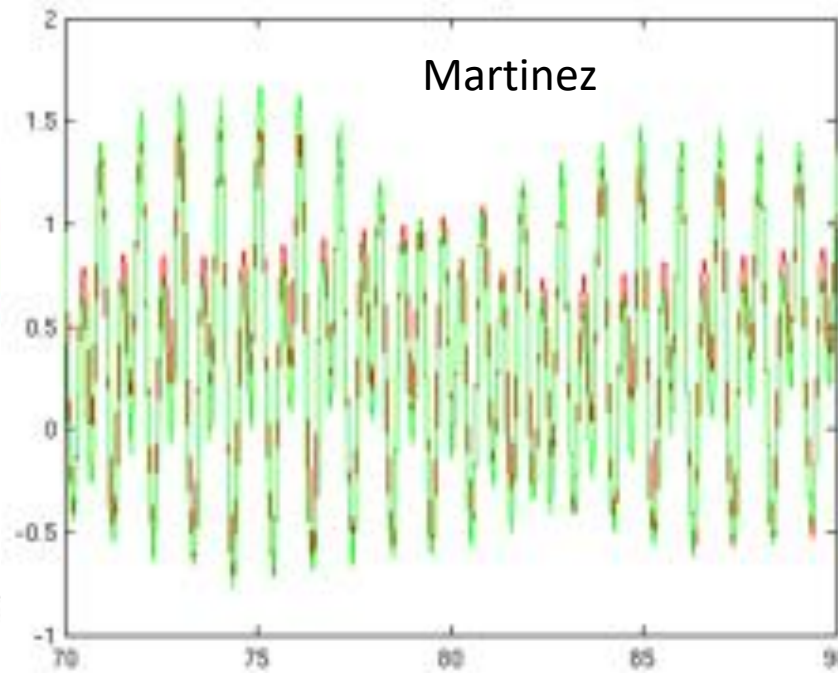
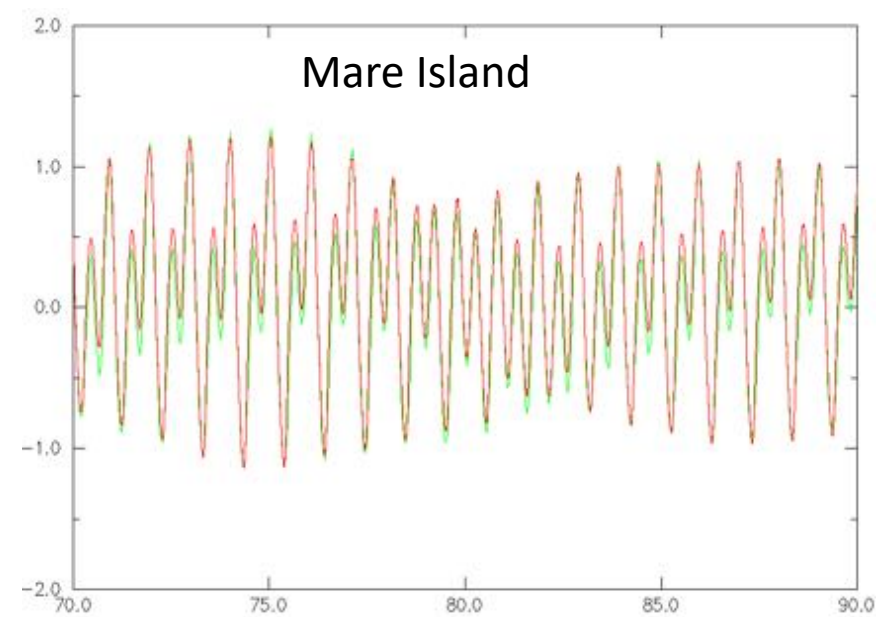
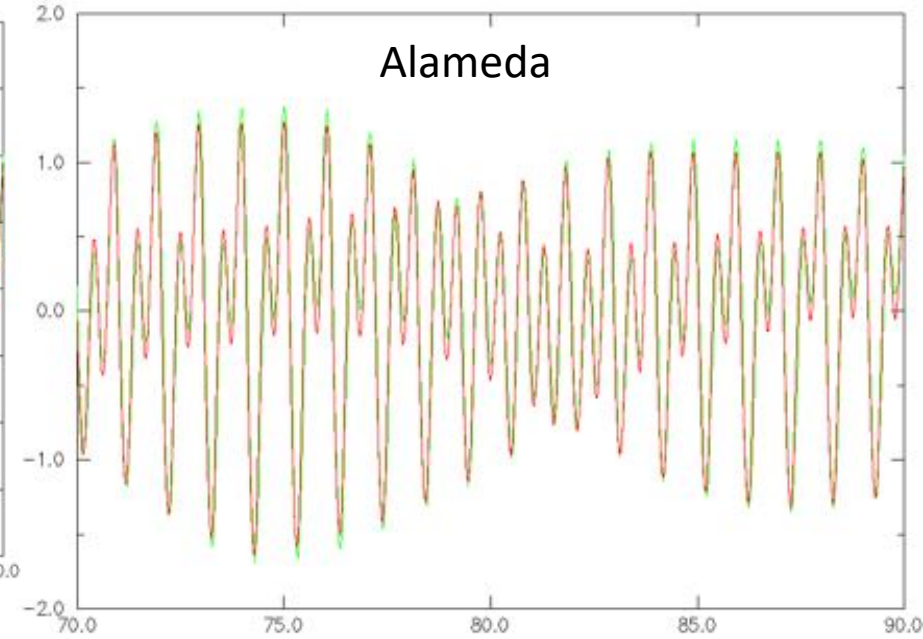
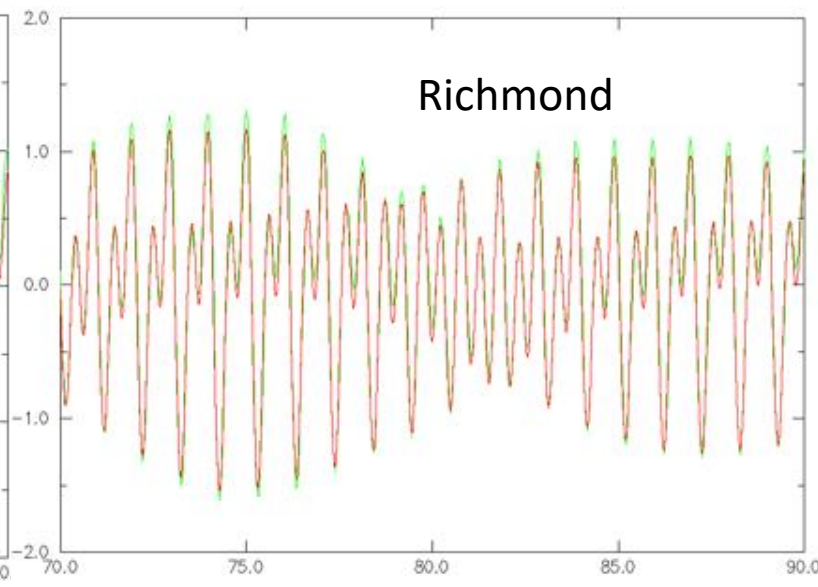
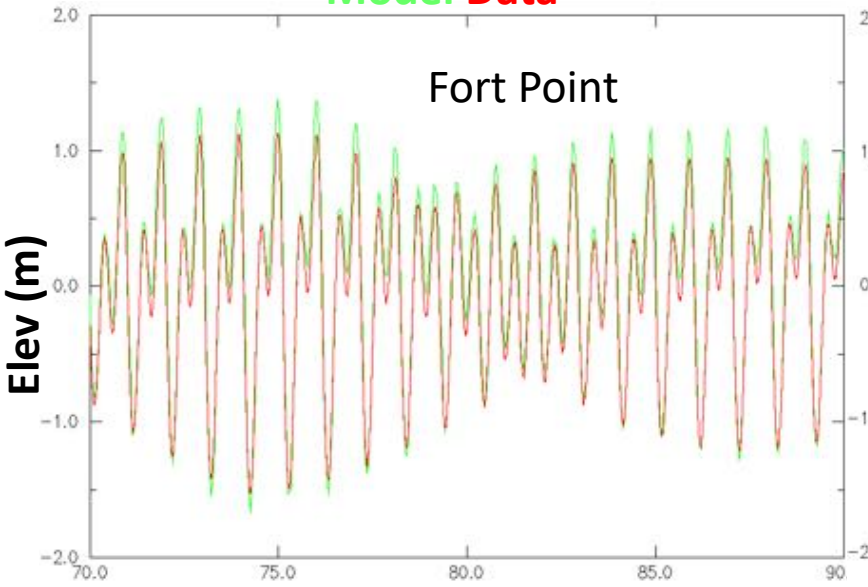
Min R = 0.00000

	#TE	%	#NBE	%	#NPE	%	#PE	%
R < 0.01	5	0.01	5	0.01	5	0.01	0	0.00
R < 0.05	17	0.02	15	0.02	15	0.02	2	200.00
R < 0.10	174	0.19	120	0.13	120	0.13	54	5400.00
R < 0.20	773	0.83	596	0.66	596	0.64	177	17700.00
R < 0.50	20920	22.38	19817	21.99	19817	21.20	1103	110300.00
R < 1.00	92085	98.53	89063	98.85	89063	95.30	3022	302200.00



Field validation (2): elevation

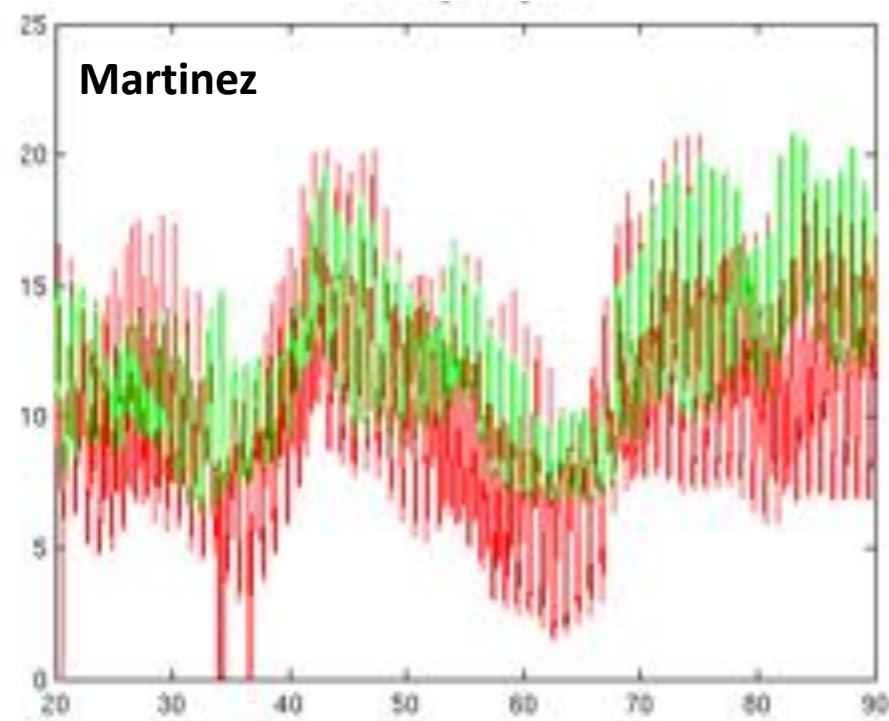
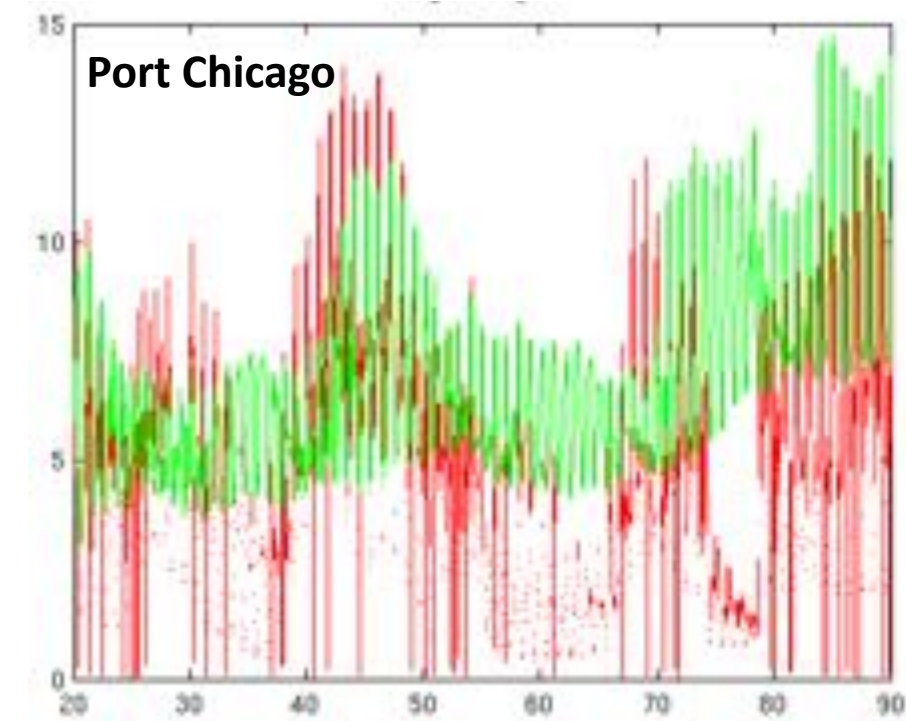
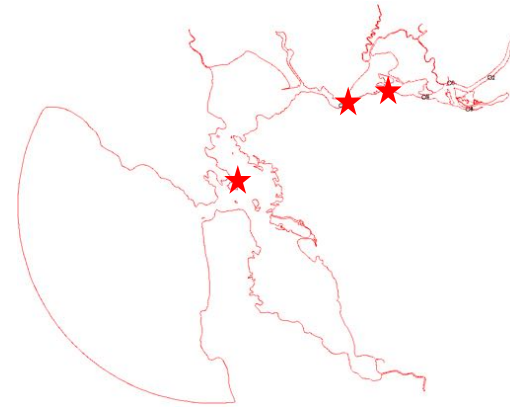
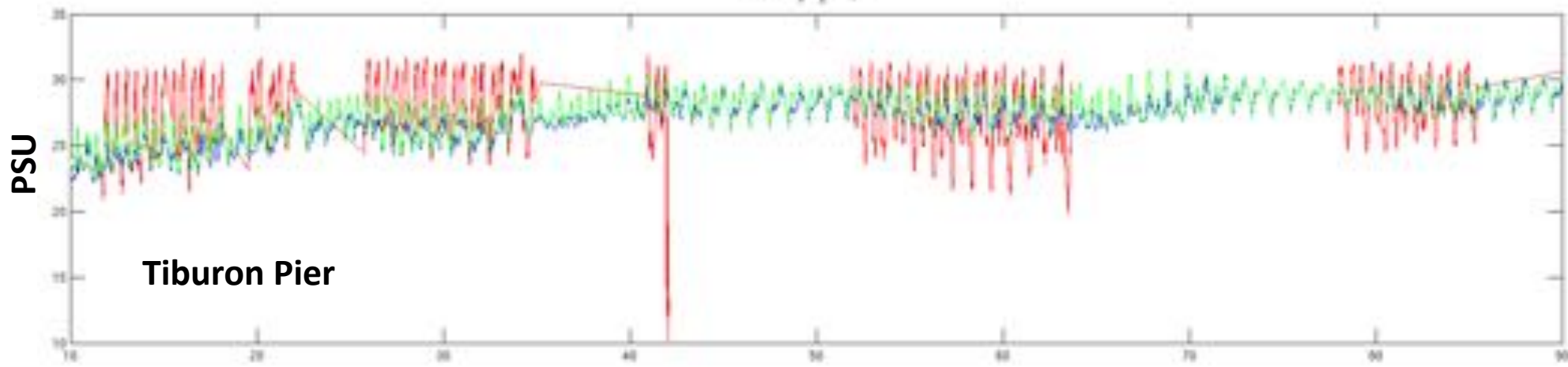
Model Data



- Tidal range is generally over-estimated
- Tide reflection is a problem...

Field validation (2): salinity

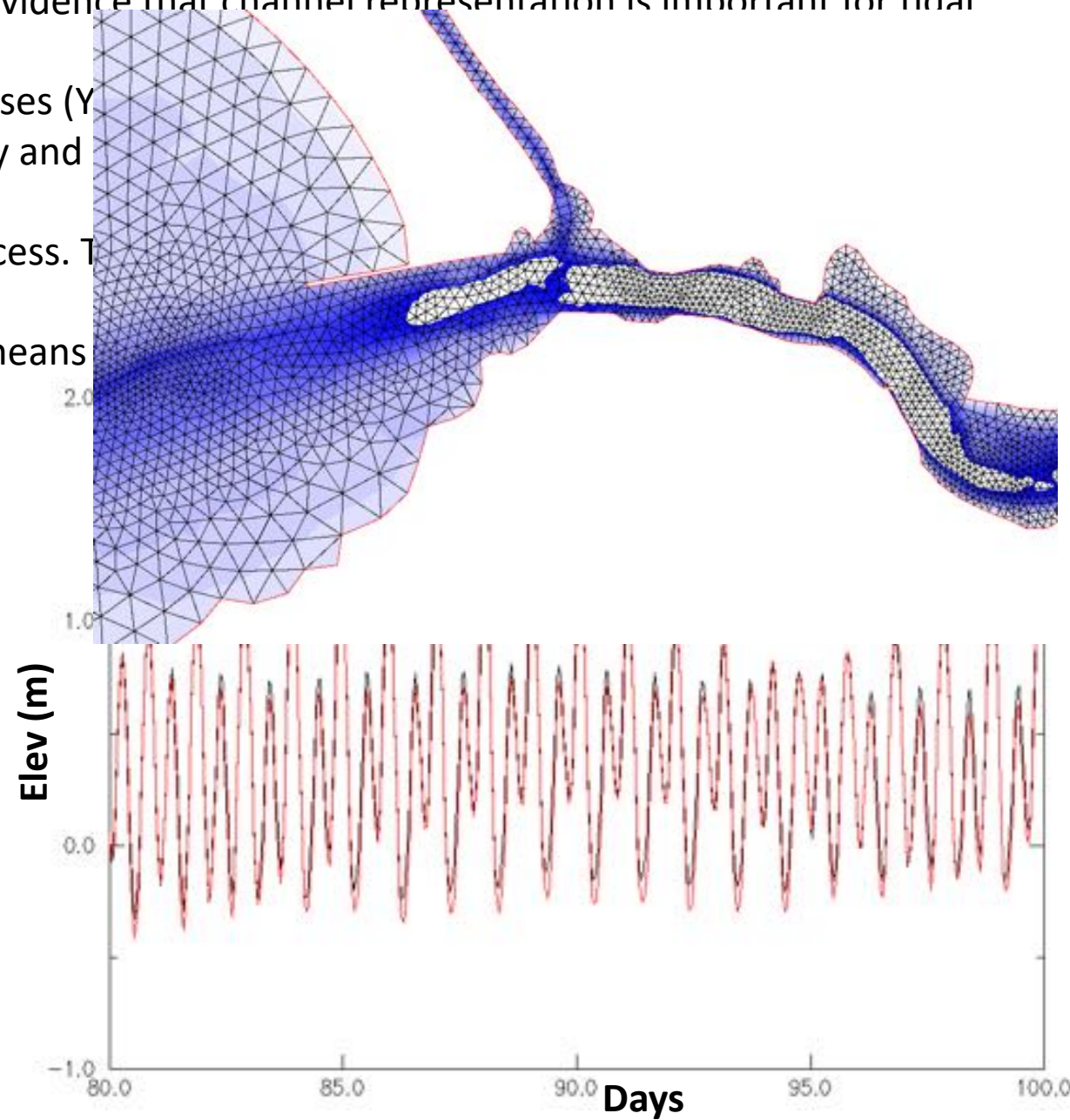
Model Data



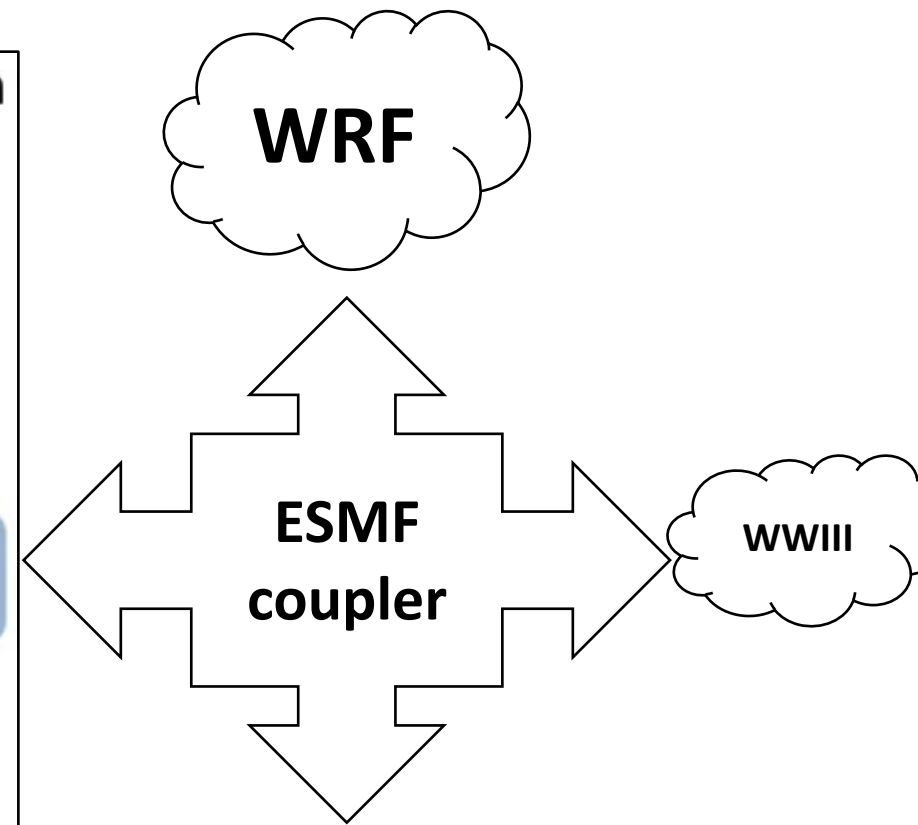
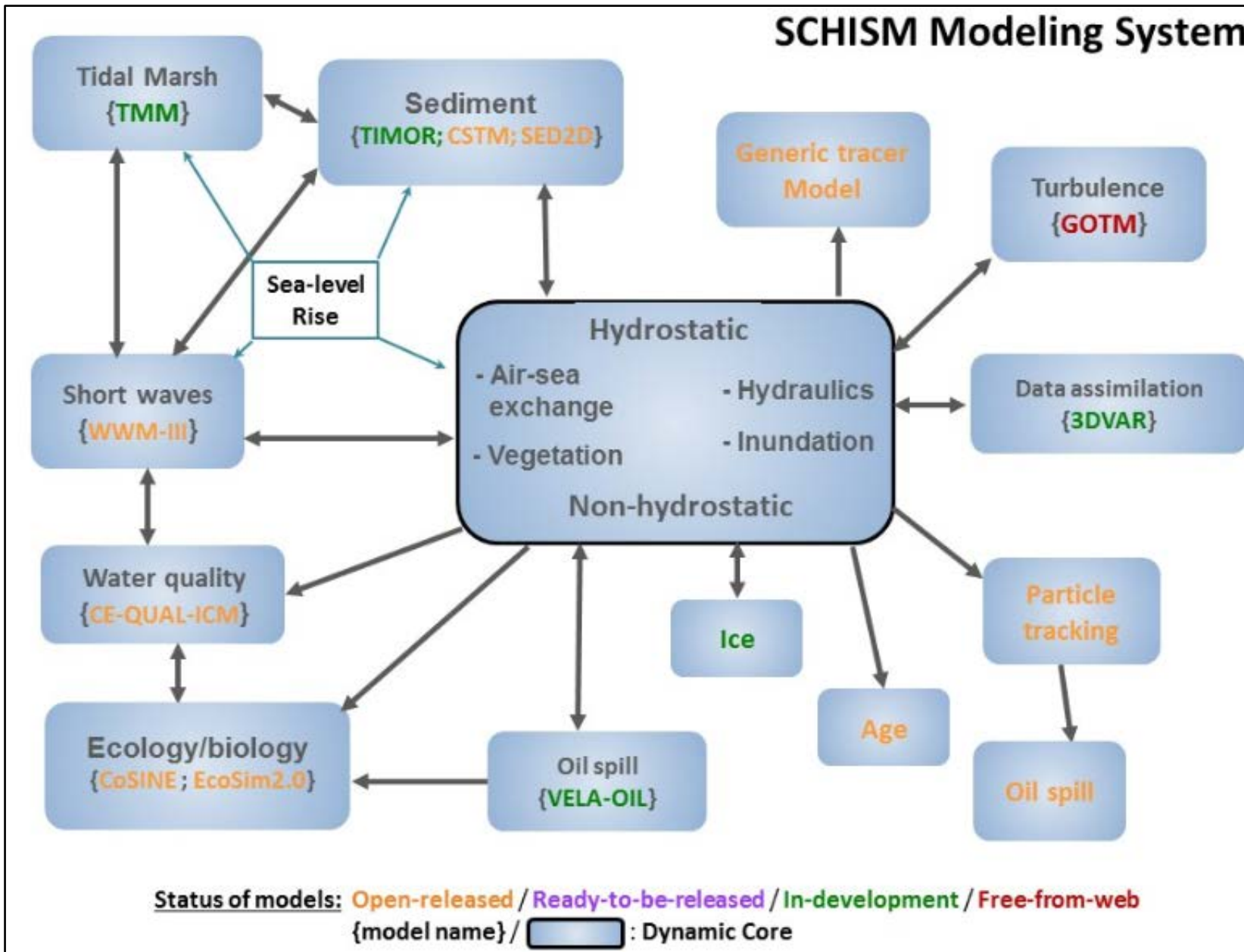
- Variability of salinity is under-estimated
- S is sensitive to closure and vertical resolution

Field validation (2): sensitivity

- * Elev results are sensitive to the # of sub divisions, which is an evidence that channel representation is important for tidal dynamics
 - * Bathymetry is the leading-order force in nearshore processes (Y
- * Unfortunately the sub-grid capability does not improve velocity and rectangular base grid ('structured grid') is not an option
- * This means grid quality is very important in the calibration process. This modestly complex geometry
 - * Gridgen for orthogonal grids can never be 'local', which means
 - * E.g. we know Carquinez Strait is a key control in this system but refining this strait would entail a non-local refinement, which may lead to degradation of results in previously calibrated areas
 - * Since the model only drives flow along normal directions, it becomes problematic in estuarine where there is often a preferential direction (e.g. channelized flow). Waves may be reflected prematurely as the flow seems to have trouble following the preferential direction. Compare this to the FE formulation in SCHISM, where there is no preferential direction



Second tide-estuary model: SCHISM

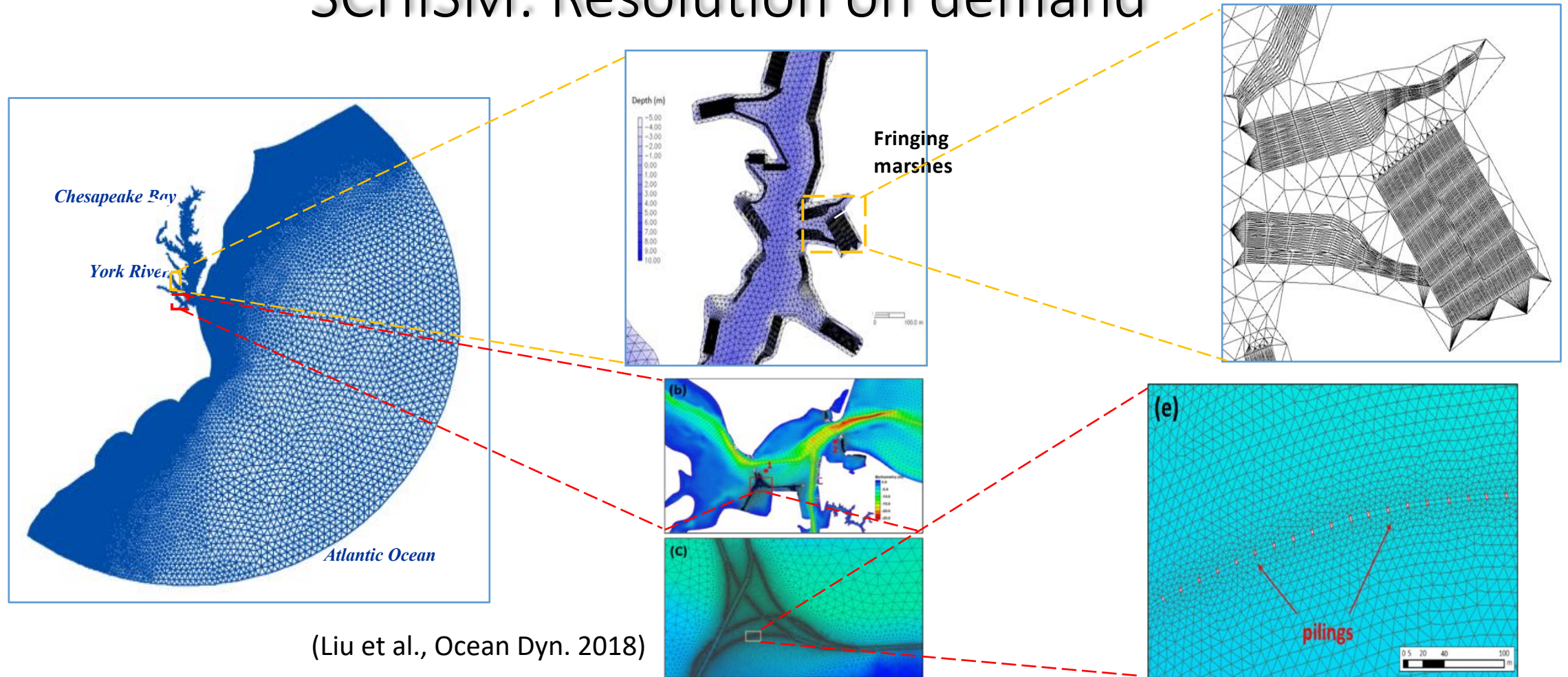


- † SCHISM is a well validated TES model
- † Has been extensively applied to estuaries and regional oceans worldwide
- † Key difference from MPAS-OI: finite element method for solving the continuity-moment equations

Why SCHISM?

- Major differentiating features
 - **No bathymetry smoothing or manipulation necessary**: faithful representation of bathymetry is key in nearshore regime (Ye et al. 2018, OM) – a lot harder when you start to apply high resolution
 - **Implicit** FE solvers → superior stability → very tolerant of bad-quality meshes (in non-eddy regime)
 - **Accurate yet efficient**: implicit + low inherent numerical dissipation (balance between numerical diffusion and dispersion); flexible 3D gridding system
 - Need for grid nesting is minimized: ‘creek to ocean’
- Well-benchmarked; certified inundation scheme for wetting and drying (NTHMP)
- Fully parallelized with domain decomposition (MPI+openMP) with good strong scaling (via PETSc solver)
- Operationally tested (DWR, EPA, NOAA, CWB ... EU)

SCHISM: Resolution on demand



- Resolution on demand is where unstructured-grid (UG) models shine
- In reality however, many challenges hinder true multi-scale modelling, many of which are numerical ones
- The implicit FE formulation in SCHISM makes it very tolerant of ‘bad’ meshes
- ‘Smooth grids’ are often too expensive and cumbersome to generate
- SCHISM’s superior stability and robustness allow high resolution to be applied anywhere *at will*

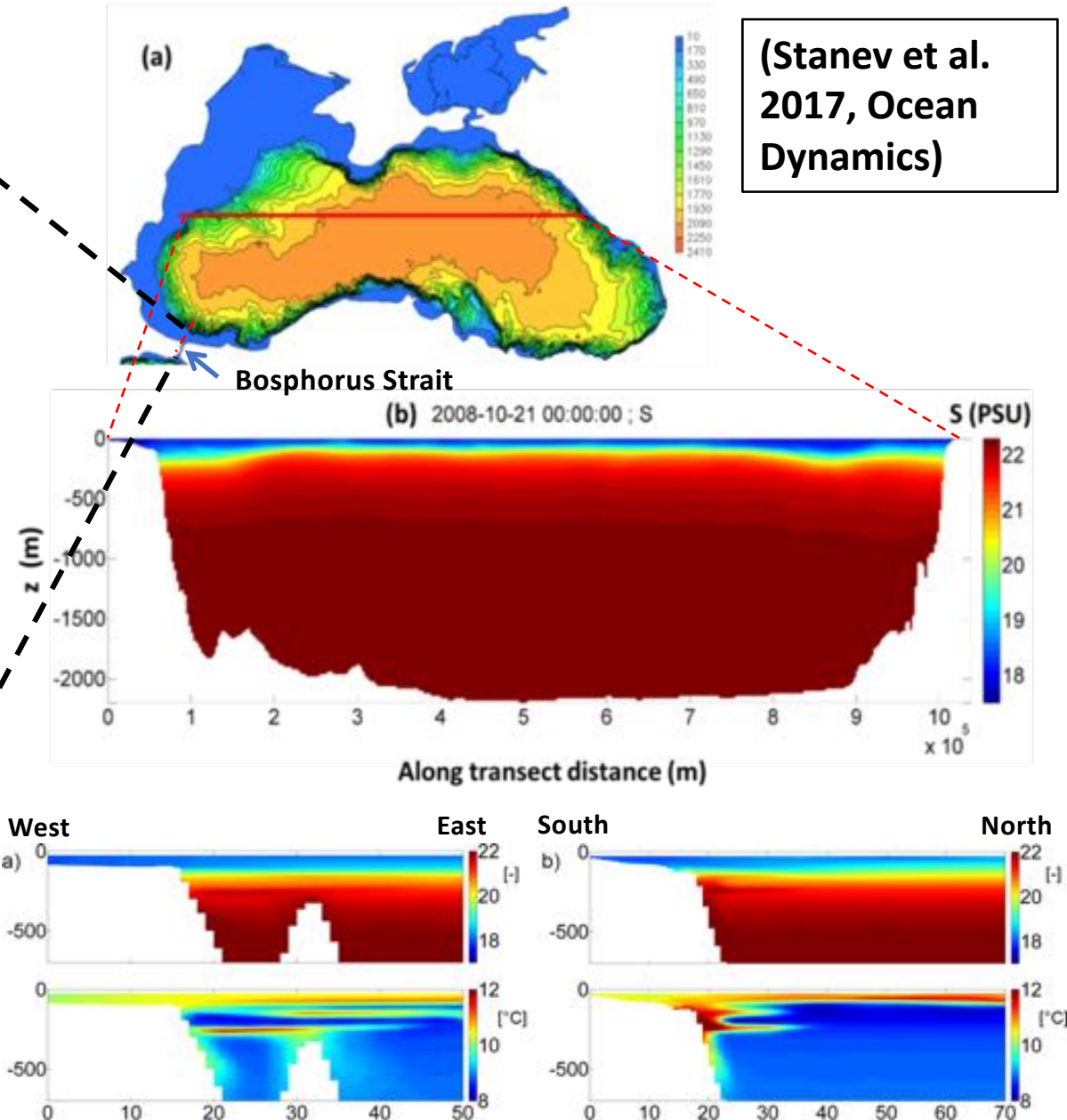
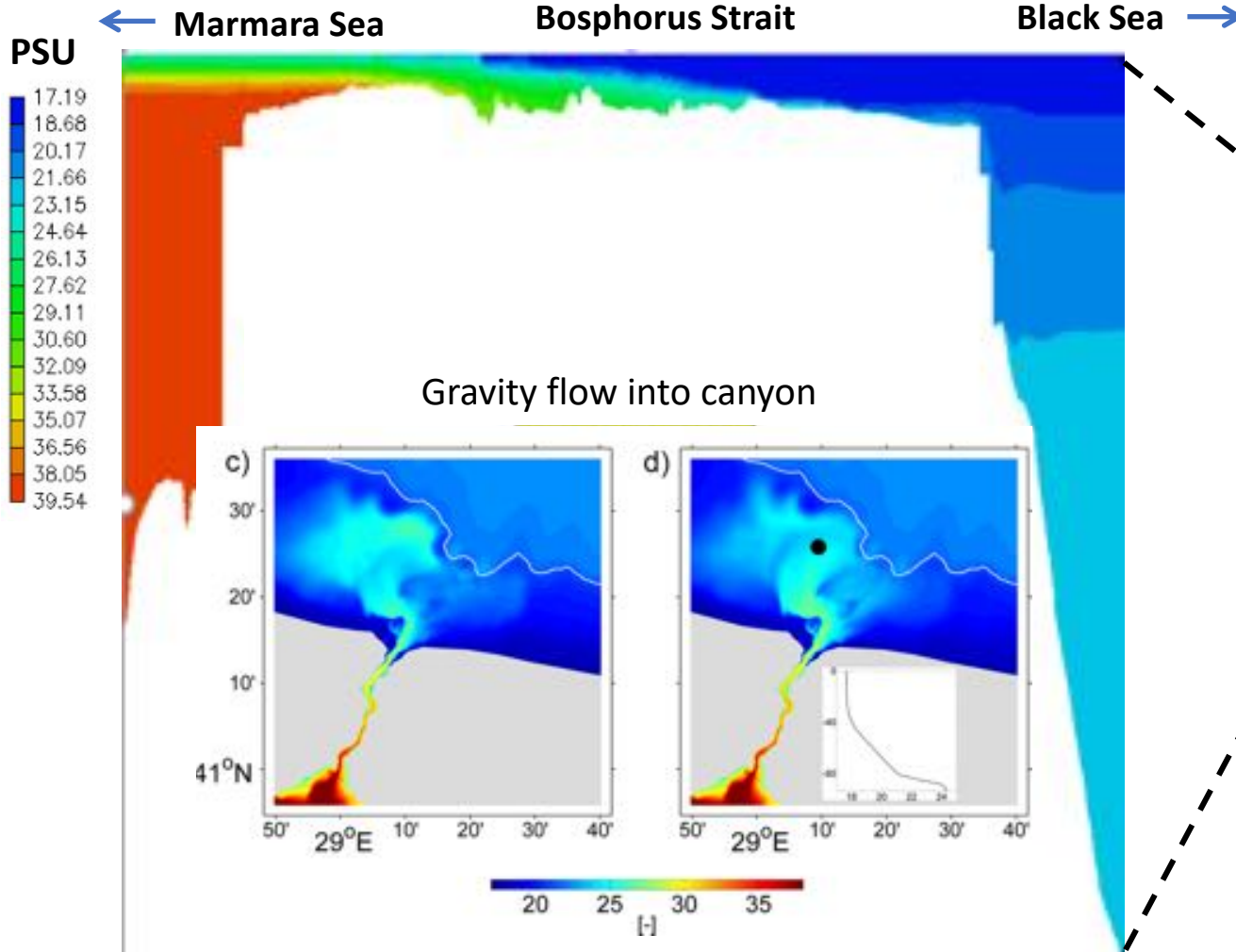
SCHISM: creek to ocean capability



- ✓ We are working on integrating oceanic processes to the model
- ✓ SCHISM's polymorphism is a huge plus. 1D/2D/3D cells in a single grid
- ✓ Despite the ultra fine resolution ($\sim 2\text{m}$) used in these applications, the model can readily represent complex features (using skew elements) as found in nature
- ✓ Vegetation effects are incorporated *implicitly* in the model and so do not require a separate land model
- ✓ We are working with EPA and CAL-DWR for water quality studies in the San Francisco Bay Area

Flow over steep bathymetry

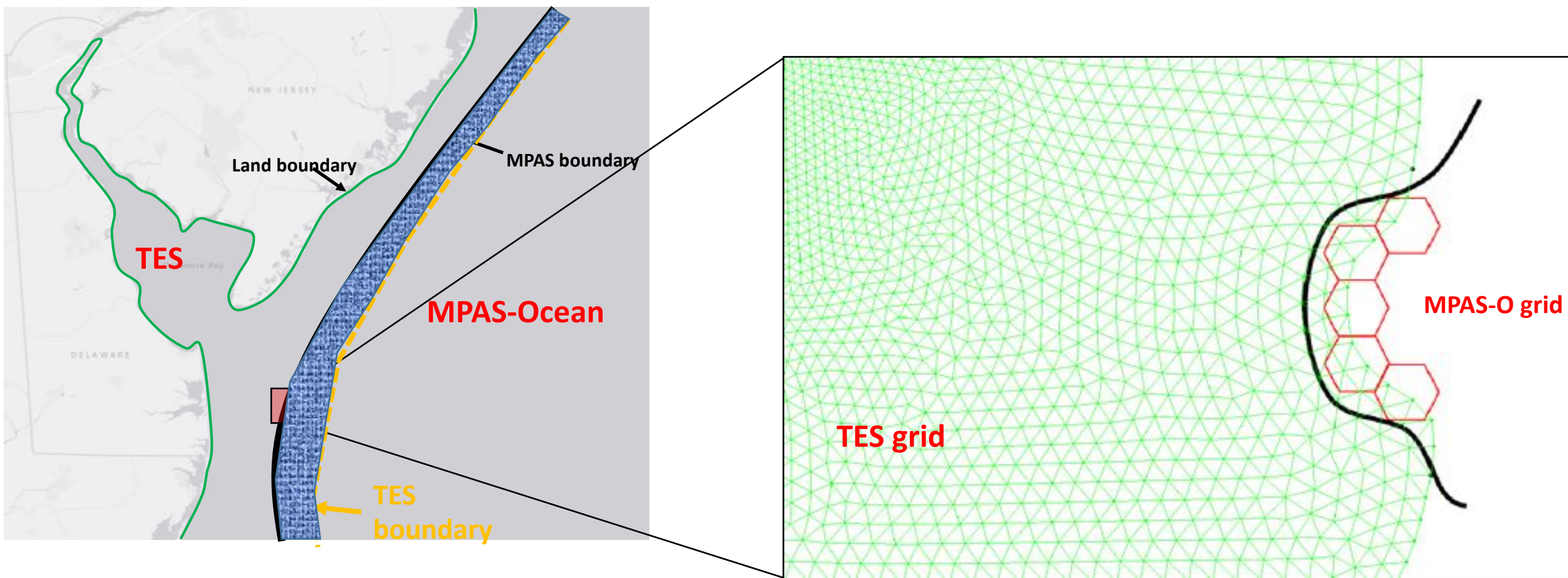
(Stanev et al.
2017, Ocean
Dynamics)



- † Either Z or terrain-following grid will have issues here
- † Steep slopes are actually common in oceans and estuaries
- † Can serve as revealing benchmarks

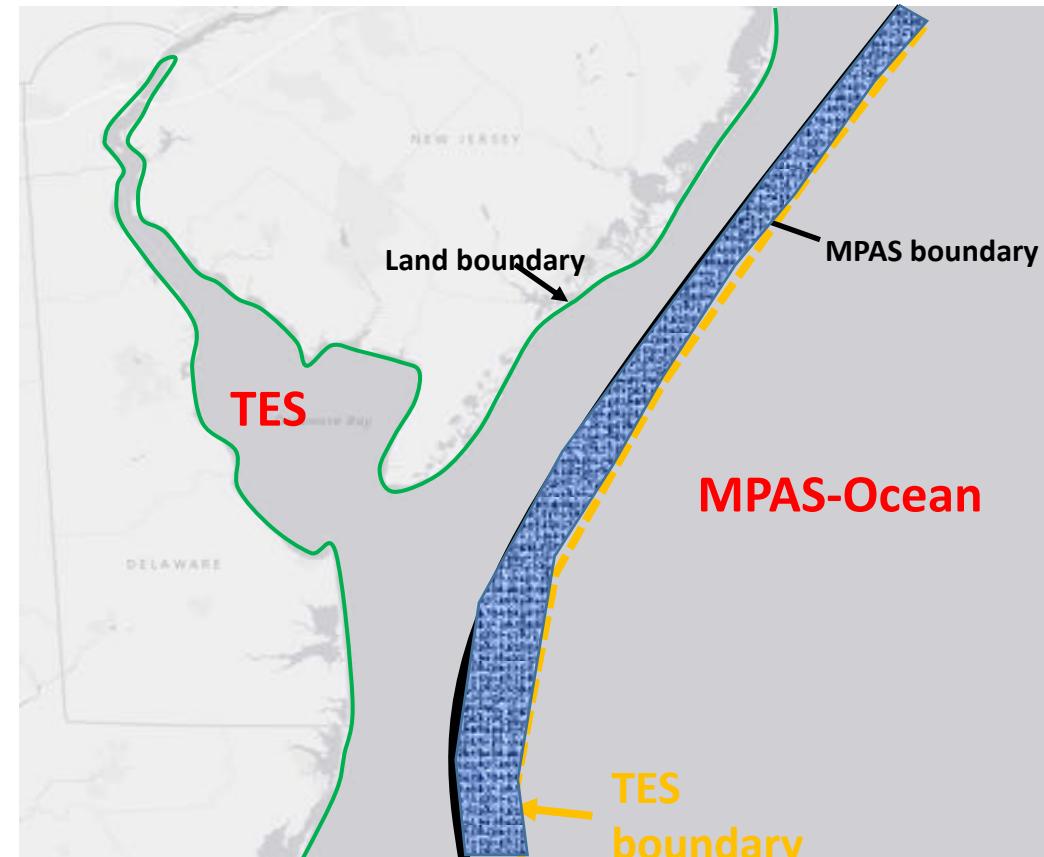
Coupling of MPAS-OI and SCHISM to MPAS-O

- TES models (MPAS-OI or SCHISM) need to be two-way coupled to global ocean model MPAS-O
- We propose a relaxation method: state variables in TES and MPAS-O are relaxed to each other in an overlapping region (more later)
- After some exploration and discussion with experts, we found that the existing E3SM coupler (CIME) is not appropriate for coupling
- SCHISM has ESMF component but MPAS-O does not.



Coupling strategy

- † MPAS-O advances certain number of steps (from t_1 to t_2), and send the info at t_1 and t_2 to SCHISM
- † SCHISM will advance same amount of time (from t_1 to t_2), using elev and velocity info from MPAS-O as boundary condition at its open boundary, with linear interpolation in time, and nudging to tracers in the overlapping zone
- † SCHISM sends back info in the overlapping zone to MPAS-O at t_2
- † MPAS-O relaxes all variables (including elev, vel) in the zone, as in a corrector step
- † MPAS-O continues the time stepping, and the process is repeated
- † Works with tides as well (MPAS-O may need a smaller time step)



Ongoing work on coupling: details

- † At Mark Petersen's suggestion, we are trying the approach of adding SCHISM as an analysis member like CVMIX to take advantage of the existing infrastructure
- † Assuming the analysis component is called by all MPI ranks. MPAS-O only uses MPI_COMM_WORLD for communication?
- † All ranks will wait for SCHISM at specified time steps (barrier, or checking SCHISM outputs...): the two models run sequentially
- † But only a subset of MPI processes will form a new comm group that calls SCHISM (which will use the new comm group). MPI_Comm_split() is used for this purpose. This is because SCHISM usually does not need so many cores
 - † Alternative would be to split the comm world for MPAS-O and SCHISM at start, but this involves changes in MPAS-O code
 - † More work would be needed to run the two models concurrently (will not pursue this)
- † Steps: some prototype code has been written
 - † For QU240 test, start with same # of cores for both models. The two can run sequentially. Tested simple message passing between the two models
 - † Next step is to use mpas_ocn_TEMPLATE.F as a template as suggested by Mark
 - † Implement split comm, and make sure the results from each model are good (without interaction)
 - † Implement interpolation in the overlapping zone and the relaxation method. We can start without tides but need to add tides to get scientifically interesting results
- † Questions for discussion
 - † Access to global & local state variables inside analysis code: elev, u,v, T,S and eventually BGC tracers
 - † Method to gather/scatter arrays
 - † Aggregate over time: need info at two steps

Summary

- We have implemented a nearshore component for MPAS-O
 - Finite-volume/finite-difference formulation on orthogonal grids with arbitrary polygonal type
 - Implicit time stepping to avoid CFL for efficiency (even with strong wetting and drying)
 - Eulerian-Lagrangian method for momentum advection to ensure robustness
 - Sub-grid representation of bathymetry and a robust nonlinear solver for mass conservative inundation: ideal for storm surge applications
 - Results are reasonable (especially if we focus on the impact on global model)
 - Requires higher resolution than SCHISM in general
 - Requires good mesh quality that's often hard to achieve with current set of tools
 - Biogeochemistry component (CoSiNE) for SCHISM and MPAS-OI has been developed and validated, including new carbon module, sediment transport, and treatment for light (not covered in this talk but Zhengui will present results at Nov meeting)
- MPAS-OI and SCHISM are being coupled to MPAS-O

Generation of orthogonal grids

❑ JANET® is a commercial software of which we have a license

- Mostly designed to generate orthogonal tri-quad grids for complex domain
- More functionalities than other packages
- Ability to use arcs is essential for feature capturing; we have ample evidence that this is very important to capture the correct volume (e.g. in a channel) for salt intrusion studies
- Newer versions have sub-grid capability
- Labor intensive and crash prone even for modest grid size, especially if quads are requested (e.g., ~1 week to generate a San Francisco Bay grid)

❑ JIGSAW

- Freeware using matlab; triangles only (Delauney → orthogonal), which can be used to generate the dual graph (hex)
- Assumes an exterior and a series of singly connected interior (island) boundaries
- If user specifies multi-connected interior boundaries, the tool will arbitrarily assign some as 'islands'. Darren promised to work on this limitation
- Given our experience with JANET, not sure how robust and how good the mesh quality will be for complex channels

